hydroxyl radical mediated DNA adduct formation and oxidative stress by the PCP metabolites. Functional symptoms, such as hyperthermia (sometimes life-threatening), profuse sweating, nausea, and uncoordinated movements were noted. Hyperthermia and other functional symptoms have been explained by the uncoupling of oxidative phosphorylation in mitochondria.

Here, we report that a comprehensive Percellome analysis revealed that PCP was the only chemical among the 111 tested in our project that strongly induced the interferon signaling gene (ISG) network. Additional pathways induced by PCP were Nrf2-mediated oxidative stress responses and other metabolic pathways more commonly seem among the 111 chemicals.

MATERIALS AND METHODS

Test chemical

PCP, standard grade (100.0% by gas chromatography coupled with flame ionization detector, Wako Pure Chemical Industries, Ltd., Tokyo, Japan) was dissolved in water containing 0.5% methyl cellulose (Shin-Etsu Chemical Co., Ltd., Tokyo, Japan).

Animal experiments

All experiments were carried out under approval of Experimental Animal Use Committee of National Institute of Health Sciences, Japan. C57BL/6 Cr Slc (Japan SLC, Inc., Shizuoka, Japan) twelve week-old male mice maintained in a barrier system with a 12 hr photoperiod were used in this study. Prior to the main study, a dose finding study was performed. This study revealed that 100 mg/kg was the maximum dose without clinical symptoms or alteration in H&E histology of the liver sampled 24 hr after single oral administration (a standard criteria for the top dose of the Percellome Project study). For the liver transcriptome experiments, forty eight mice were divided into four groups with twelve each, and given a single dose of PCP at 0, 10, 30 and 100 mg/kg by oral gavage. At 2, 4, 8 and 24 hr post-gavage, three randomly selected mice from each dose groups were euthanized by exsanguination under ether anesthesia and the livers were excised into ice-cooled plastic dishes. Tissue blocks weighing 30 to 60 mg were placed in an RNase-free 2 ml plastic tube (Eppendorf GmbH., Hamburg, Germany) and soaked in RNAlater (Ambion Inc., Austin, TX, USA) within 3 min of the beginning of anesthesia. The 12 animal sampling for each time point was finished within 25 to 30 min in order to avoid circadian-based variation within a time point.

Sample preparation and GeneChip measurement

The tissue blocks soaked in RNAlater were kept overnight at 4°C or until use. RNAlater was replaced in the 2 ml plastic tube with 1.0 ml of RLT buffer (Qiagen GmbH., Hilden, Germany), and the tissue was homogenized by adding a 5 mm diameter Zirconium bead (Funakoshi, Tokyo, Japan) and shaking with a MixerMill 300 (Qiagen GmbH) at a speed of 20Hz for 5 min (only the outermost row of the shaker box was used).

Three separate 10μl aliquots were taken from each sample homogenate to another tube and mixed thoroughly. A final 10 μl aliquot there from was treated with DNAse-free RNase A (Nippon Gene Inc., Tokyo, Japan) for 30 min at 37°C, followed by Proteinase K (Roche Diagnostics GmbH., Mannheim, Germany) for 3 hr at 55°C in 1.5 ml capped tubes. The aliquot was transferred to a 96-well black plate. PicoGreen fluorescent dye (Molecular Probes Inc., Eugene, OR, USA) was added to each well, shaken for 10 sec four times and then incubated for 2 min at 30°C. The DNA concentration was measured using a 96 well fluorescence plate reader with excitation at 485 nm and emission at 538 nm. λ phage DNA (PicoGreen Kit, Molecular Probes Inc.) was used as standard.

As reported previously, the graded-dose spike cocktail (GSC) made of the following five *Bacillus subtilis* RNA sequences were selected from the gene list of Affymetrix GeneChip arrays (AFFX-ThrX-3_at, AFFX-LysX-3_at, AFFX-PheX-3_at, AFFX-DapX-3_at, and AFFX-TrpnX-3_at) present in the MOE430 arrays was added to the sample homogenates in proportion to their DNA concentrations (Kanno *et al.*, 2006). Then, the sample homogenates spiked with GSC were processed according to the Affymetrix standard protocol. The GeneChips used were Mouse 430 2.0. We used the in house developed SCal4 (Spike Calculation version 4, by K.A.) to check the efficiency of *in vitro* transcription, and the dose-response linearity of the five GSC spikes and to produce Percellome data, i.e. absolutized mRNA copy numbers of each PS were generated.

The data consist of four dose levels and four time points, generating a 4 x 4 matrix. The mean value (m) with standard deviation (sd) was calculated from the triplicates for all of the probe sets (PSs) for each dose-time points. In order to better visualize the changes at 2 hr, the vehicle value was used for putative zero point, and drawn a 5 x 4 surface three-dimension (3D) surface graph with X-axis for dose, Y for time, and Z for expression as shown in Fig. 1.

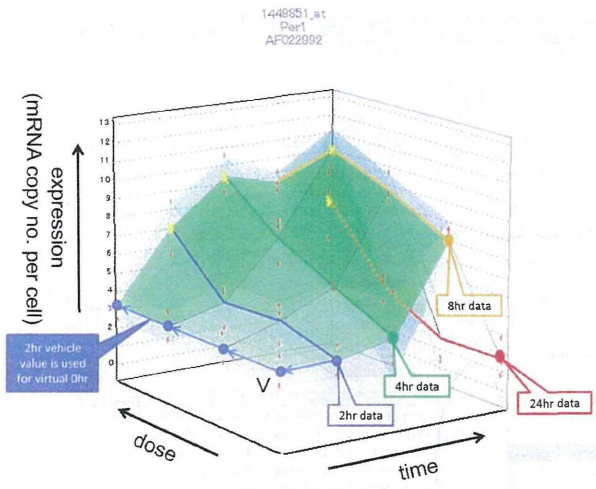

Fig. 1. Three dimensional surface expressions of Percellome Project data: The project data consist of four dose levels and four time points, generating 4 x 4 matrix. The mean value and standard deviation were calculated from the triplicate data. In order to better visualize the changes at 2 hr, the vehicle value was used for zero hour data to draw a 5 x 4 surface graph with X-axis for dose, Y for time, and Z for expression. Here, Affymetrix ID 1449851_at (Per1, period homolog 1) is shown. The 5 x 4 mesh made by the mean values was painted in translucent green (mean surface). The mean surface is rainbow-colored from blue, green, red to yellow according to its peak absolute values (cf. Fig. 3, Supplementary Fig. 1). Above and below the mean surface, +1sd and -1sd surfaces were overlaid using transparent blue. The dose-response curve at 2 hr, 4 hr, 8 hr and 24 hr are highlighted in blue, green, yellow and red. In a direction perpendicular to the dose-response curves, time course of each dose groups and vehicle group is indicated (not highlighted). The graph reads that the highest dose peaked at 4 hr at around 9 copies per cell; the middle dose peaked at 8 hr above 10 copies per cell. The vehicle group (V) showed the circadian change and peaked at 8 hr. The small red crosses are data of each animal sample (n = 3). Yellow asterisks indicate that the marked mean values were significantly different from concurrent vehicle value by $p < 0.05$ (Student's t-test).

Comprehensive selection of treatment-responding mRNAs

The in house developed software, RSort (Roughness Sort by K.A.) was used for automatic selection of treatment-responding mRNAs. This program sorts the PSs based on the roughness of the 3D surface. In other words, calculate the numbers of peaks (upward and downward) in a surface and sort by the number of peaks (maximum of eight peaks in 4 x 4 grid of the surface). Next, it filters the PSs by the number of peaks (normally three or less peaks) and additional parameters such as maximum expression level (normally more than one copy per cell for liver samples), p values between vehicle and top dose groups ($P < 0.05$ or $p < 0.01$). Here, a surface was selected when it had three peaks or less, the first peak in high doses (at any time) or the first peak in middle doses if its value is not significantly different from the neighboring high dose at $p < 0.01$ by Student's t-test, and the value of the peak is significantly different from that of vehicle control at $p < 0.05$ by Student's t-test. These automatically selected PSs were then visually checked for their 3D-surface shapes (to eliminate noisy data), and subdivided into those showed initial changes at 2, 4, 8, and 24 hr. A cross-referencing program named PE (Percellome Explorer, by K.A.) was used to select a list of chemicals that share PSs common to the visually confirmed list of PCP. The PE contains the gene lists automatically selected by the RSort of all data in our Percellome Project (168 datasets for liver samples, 286 for all samples), and automatically cross-refers and sorts out the chemicals sharing the same PSs (Fig. 2). The automatically selected gene lists (product sets) were visually checked to remove noise surfaces.

In Situ Hybridization

For *in situ* hybridization of Irf7 and Stat1 mRNAs, QuantiGeneViewRNA ISH Tissue Assay kit (Affymetrix, Inc., Santa Clara, CA, USA) was used. The probes were designed and synthesized by Affymetrix; regions covered were 2-1461 bases for Irf7 and 707-1710 bases for Stat1. 10% buffered formalin fixed liver tissues were dehydrated and embedded in paraffin. Tissue sections were mounted on "FRONTIER coated glass slides" (Matsunami Glass Ind., Ltd. Osaka, Japan). The slides were completely dried and stored until use. The slides were re-fixed in 10% formaldehyde for 1 hr at room temperature and washed with PBS and deparaffinized with xylene, pretreated in 1x Pretreatment Solution at 98°C for 30 min and digested with Protease QF at 40°C for 20 min. The probes were hybridized at 40°C for 2 hr and the signals were detected with Fast Red.

RESULTS

The numbers of PSs that started to change in response to PCP treatment at 2, 4, 8 and 24 hr were 98, 55, 127 and 1192 respectively (Supplementary Table 2, Supplementary Fig. 1). Chemicals or treatment in the Percellome database (Supplementary Table 1), that shared the PS list with PCP are shown in Table 1. The chemicals that shared the most with the 2 hr PS list of PCP

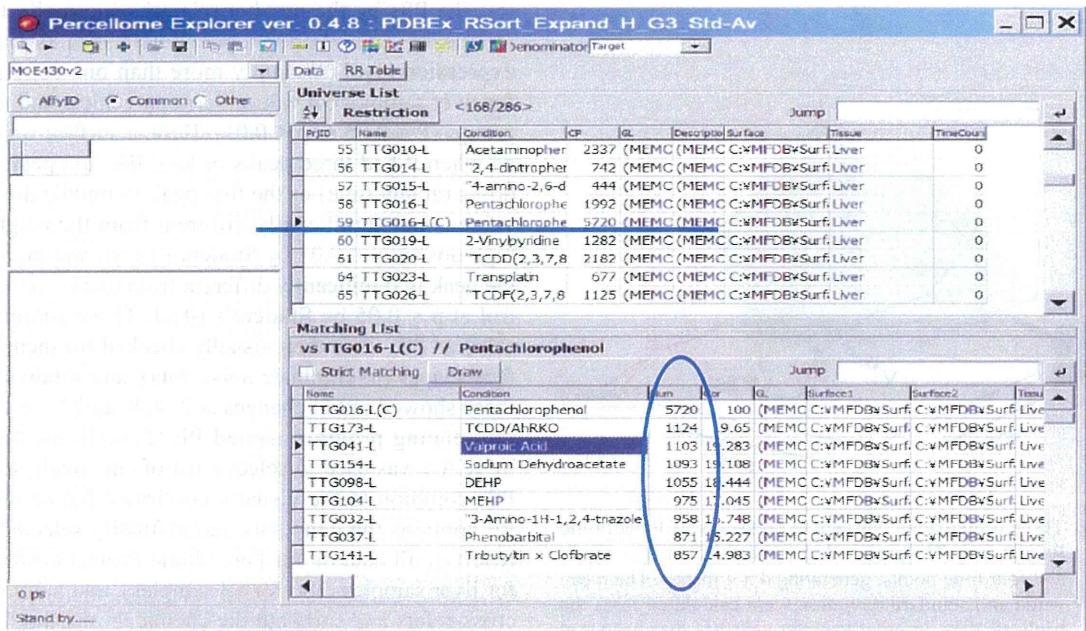

Fig. 2. PercellomeExplorer (PE) Software: The PE contains the gene lists automatically selected by the RSort software program of all data in our Percellome Project (168 datasets for liver samples, 286 for all samples, as of May 2013), and automatically picks up the chemicals sharing same PSs. TTG016-L(C), the study code for PCP was selected from the upper window and the chemicals sharing the PSs were listed in the lower window. These lists await visual confirmation.

was sodium dihydroacetate (TTG154-L); 51 PSs, followed by acephate (TTG109-L); 24 PSs, down to 5-fluorouracil (TTG160-L); 4 PSs. The sum set (or union of sets in set theory) of the 2 hr PS lists that are listed in the 2 hr column of the Table 1 contained 75 PSs (up-regulated (Up) 59, down-regulated (D) 16). Likewise, the sum set of the 4 hr PS lists contained 31 PSs (Up 22, D 9), 8 hr 46 PSs (Up 23, D 23) and 24 hr 636 PSs (all Up). The PS list unique to PCP (Unique list) at each time point contained 23, 24, 81, and 556 PSs at each time points (cf. Supplementary Table 2).

Profiles of genes changed at 2, 4 and 8 hr

The PS list common to other chemicals (Common list) contained the gluconeogenesis pathway of PGC-1A (Ppargc1a)/Foxo1/HNF4 (Puigserver *et al.*, 2003) that were induced at 2 hr (Fig. 3). This finding is in concordance with the report in experimental animals that PCP acutely induces hyperglycemia (Deichman *et al.*, 1942; Clayton and Clayton, 1981). Ppargc1a was reported to increase the expression of Lpin1 (Finck *et al.*, 2006), which was also the case here. A small set of genes encoding metabolic enzymes was induced during the first 8 hr, including Cyp2a4, Cyp4f16, Cyp7a1, Cyp17a1, Cyp39a1, Fmo2, and Fmo5 (Fig. 3).

Ingenuity pathway analysis (Ingenuity Systems, Inc. Redwood City, CA, USA) indicated that these genes are likely to be induced by Nr1i3 (CAR), Nr1i2 (PXR/SXR) or Nr5a1 (data not shown). Although our RSort program did not identify these nuclear receptors, manual search showed that PXR/SXR was induced by PCP (Fig. 3). These changes were not unique to PCP and shared by some of the chemicals in the Common list (cf. Supplementary Table 2).

Down regulation of Fos and JunB at 2, 4, and 8 hr (Fig. 3) was uniquely found in the PCP gene list. Bioinformatic analysis did not identify any associated pathways.

Profiles of genes started to change at 24 hr

The list of PSs induced at 24 hr contained two large networks. About half of the PSs showing altered expression by PCP were assigned to the interferon signaling pathway (Fig. 4, Supplementary Fig. 1). The interferon signaling genes (ISG) were highly up-regulated from Stat1, Stat2, Tyk, to Irf7, Myd88, Oas, Ifit, Cxcl10 and other downstream targets. Toll like receptors (TLRs) and

Table 1. The total numbers of probesets induced by PCP at each time points and those shared with other chemicals.

2 hr			4 hr			8 hr			24 hr		
Percellome No.	Treatment	PS	Percellome No.	Treatment	PS	Percellome No.	Treatment	PS	Percellome No.	Treatment	PS
TTG016-L(C)	Pentachlorophenol	98	TTG016-L(C)	Pentachlorophenol	55	TTG016-L(C)	Pentachlorophenol	127	TTG016-L(C)	Pentachlorophenol	1192
TTG154-L	Sodium Dehydroacetate	51	TTG104-L	MEHP	21	TTG098-L	DEHP	15	TTG098-L	DEHP	258
TTG109-L	Acephate	24	TTG098-L	DEHP	16	TTG041-L	Valproic Acid	14	TTG032-L	3-Amino-1H-1,2,4-triazole	212
TTG059-L	Caffeine	19	TTG037-L	Phenobarbital	14	TTG104-L	MEHP	14	TTG104-L	MEHP	177
TTG062-L(C)	Dexamethasone	18	TTG032-L	3-Amino-1H-1,2,4-triazole	12	TTG109-L	Acephate	13	TTG037-L	Phenobarbital	160
TTG041-L	Valproic Acid	18	TTG144-L	Tributyltin x Phenobarbital	12	TTG160-L	5-fluorouracil	10	TTG041-L	Valproic Acid	109
TTG098-L	DEHP	17	TTG150-L	Valproic acid sodium salt x Thalidomide	8	TTG154-L	Sodium Dehydroacetate	9	TTG157-L	Valproic acid sodium salt	103
TTG019-L	2-Vinylpyridine	15	TTG141-L	Tributyltin x Clofibrate	8	TTG141-L	Tributyltin x Clofibrate	8	TTG031-L	2-Chloro-4,6-dimethylaniline	94
TTG104-L	MEHP	12	TTG074-L	Bromobenzene	8	TTG031-L	2-Chloro-4,6-dimethylaniline	8	TTG154-L	Sodium Dehydroacetate	77
TTG165-L	Chlorpyrifos	12	TTG151-L	Valproic acid sodium salt x Valproic acid sodium salt	7	TTG032-L	3-Amino-1H-1,2,4-triazole	8	TTG162-L	Sesame seed oil unsaponified matter	71
TTG034-L	4-Ethylnitrobenzene	12	TTG031-L	2-Chloro-4,6-dimethylaniline	7	TTG146-L	Forskolin	6	TTG044-L	Clofibrate	69
TTG166-L	Carbaryl	10	TTG044-L	Clofibrate	6	TTG062-L(C)	Dexamethasone	6	TTG074-L	Bromobenzene	47
TTG031-L	2-Chloro-4,6-dimethylaniline	10	TTG162-L	Sesame seed oil unsaponified matter	5	TTG054-L	Diethylnitrosamine (C57BL/6)	5	TTG109-L	Acephate	17
TTG141-L	Tributyltin x Clofibrate	9				TTG132-L	Curcumin	3	TTG160-L	5-fluorouracil	13
TTG032-L	3-Amino-1H-1,2,4-triazole	9				TTG136-L	Phytol	2			
TTG027-L	1,2,3-Triazole	9									
TTG160-L	5-fluorouracil	4									
	Sum Set (common)	75		Sum Set (common)	31		Sum Set (common)	46		Sum Set (common)	636
	Sum Set (Up)	59		Sum Set (Up)	22		Sum Set (Up)	23		Sum Set (Up)	636
	Sum Set (Dn)	16		Sum Set (Dn)	9		Sum Set (Dn)	23		Sum Set (Dn)	0
	PCP NOT Sum (unique to PCP)	23		PCP NOT Sum (unique to PCP)	24		PCP NOT Sum (unique to PCP)	81		PCP NOT Sum (unique to PCP)	556

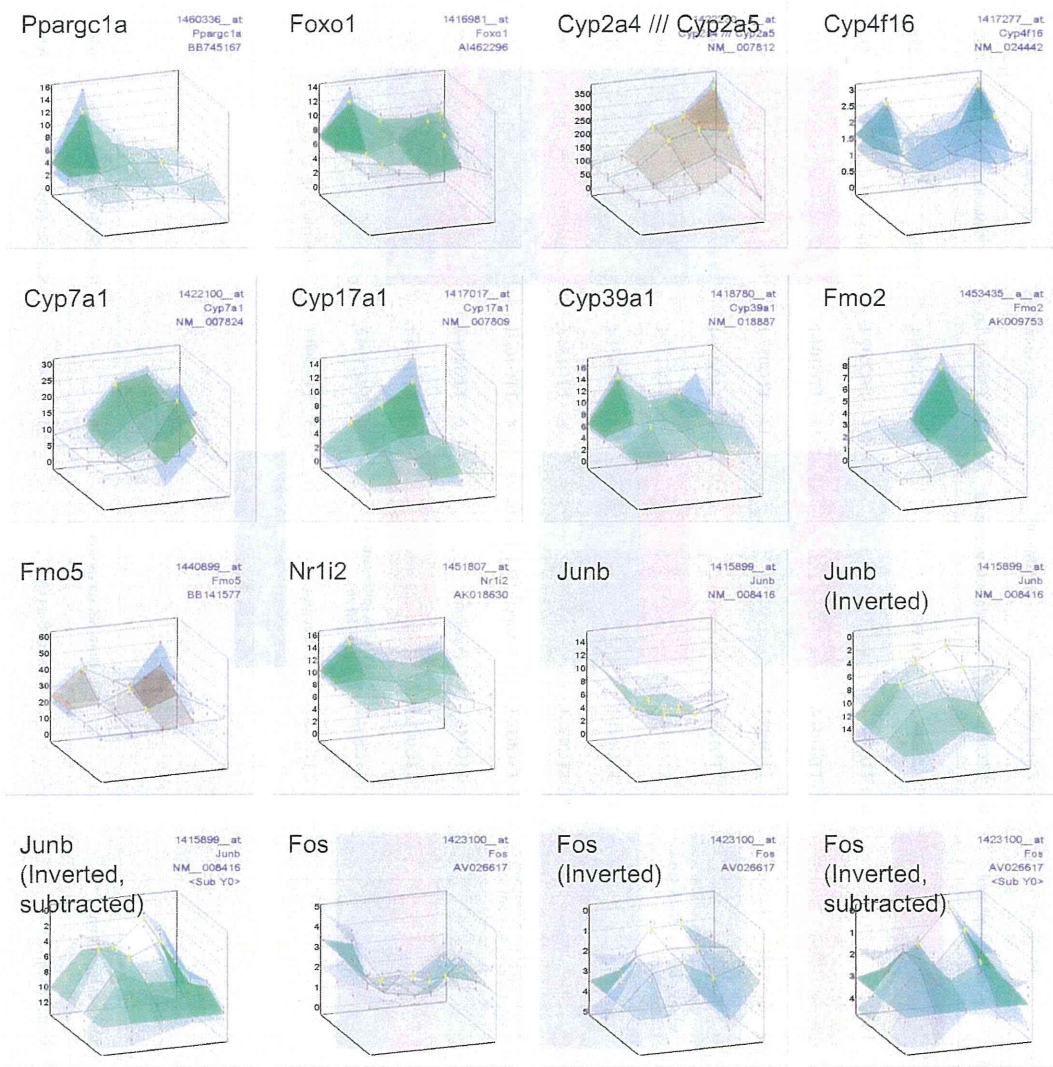

Fig. 3. Representative surface data of PSs induced at 2, 4 and 8 hr after PCP single gavage: Ppargc1a and Foxo1 are the members of gluconeogenesis pathway. A small set of genes of metabolic enzymes, such as Cyp2a4, Cyp4f16, Cyp7a1, Cyp17a1, Cyp39a1, Fmo2, and Fmo5 are induced during the first 8 hr. Nr1i2 or PXR/SXR is also induced. Down regulation of JunB and Fos at 2, 4, and 8 hr are noted. The graphs marked with (Inverted) are plotted with inverted z-axis, zero on top for better indication of suppression. The graphs with (Inverted, subtracted) are plotted, in addition to inverted z-axis, with the 2, 4, 8 and 24 hr values compensated by concurrent vehicle values so that the vehicle line is straight and cancels out the circadian changes.

other pattern recognition receptors (PRR), interferon regulatory factors (Irf) and interferon (Ifn) itself were included. These ISGs were uniquely induced by PCP. It is notable that inflammatory cytokines such as Tnf-α, IL-12 and CD40 were not effectively induced by PCP. The Ingenuity Pathways also plotted many genes in the interferon signaling with a very high probability score (Fig. 6).

In situ hybridization confirmed that hepatocytes were producing the Irf7 and Stat1 in a dose dependent manner (Fig. 7, only vehicle and top dose were shown).

The other half was assigned, by Ingeunity Pathway analysis, to Nrf2-mediated Oxidative Stress Responses

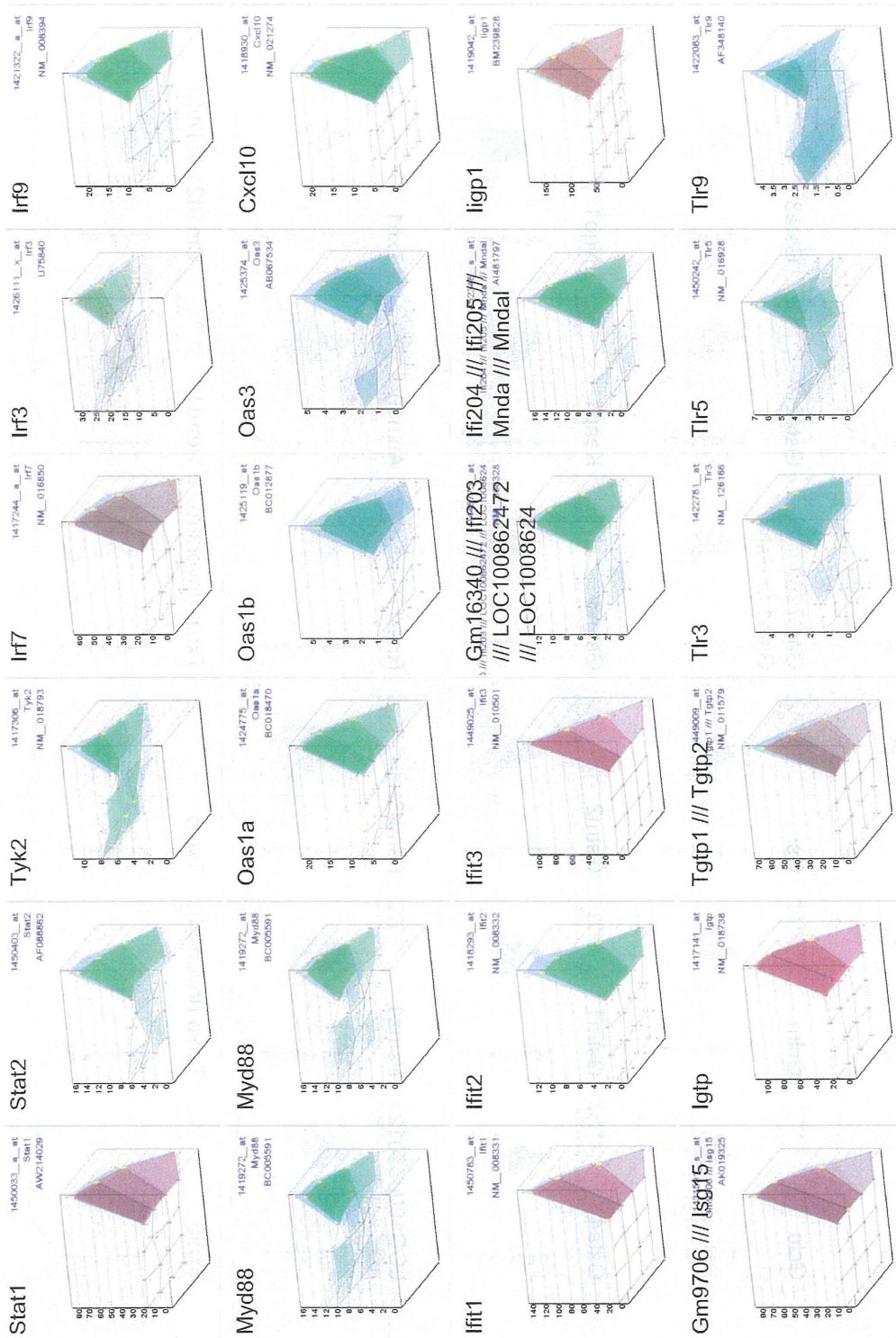

Fig. 4. Surface data of ISGs: Among about 1,200 PSs induced at 24 hr, half of them were uniquely induced by PCP and were assigned to ISG pathway from Stat1, Stat2, Tyk, to Irf7, Myd88, Oas, Ifit, Cxcl10 and other downstream targets. Some Tlrs were also uniquely up-regulated (cf. Supplementary Table 2).

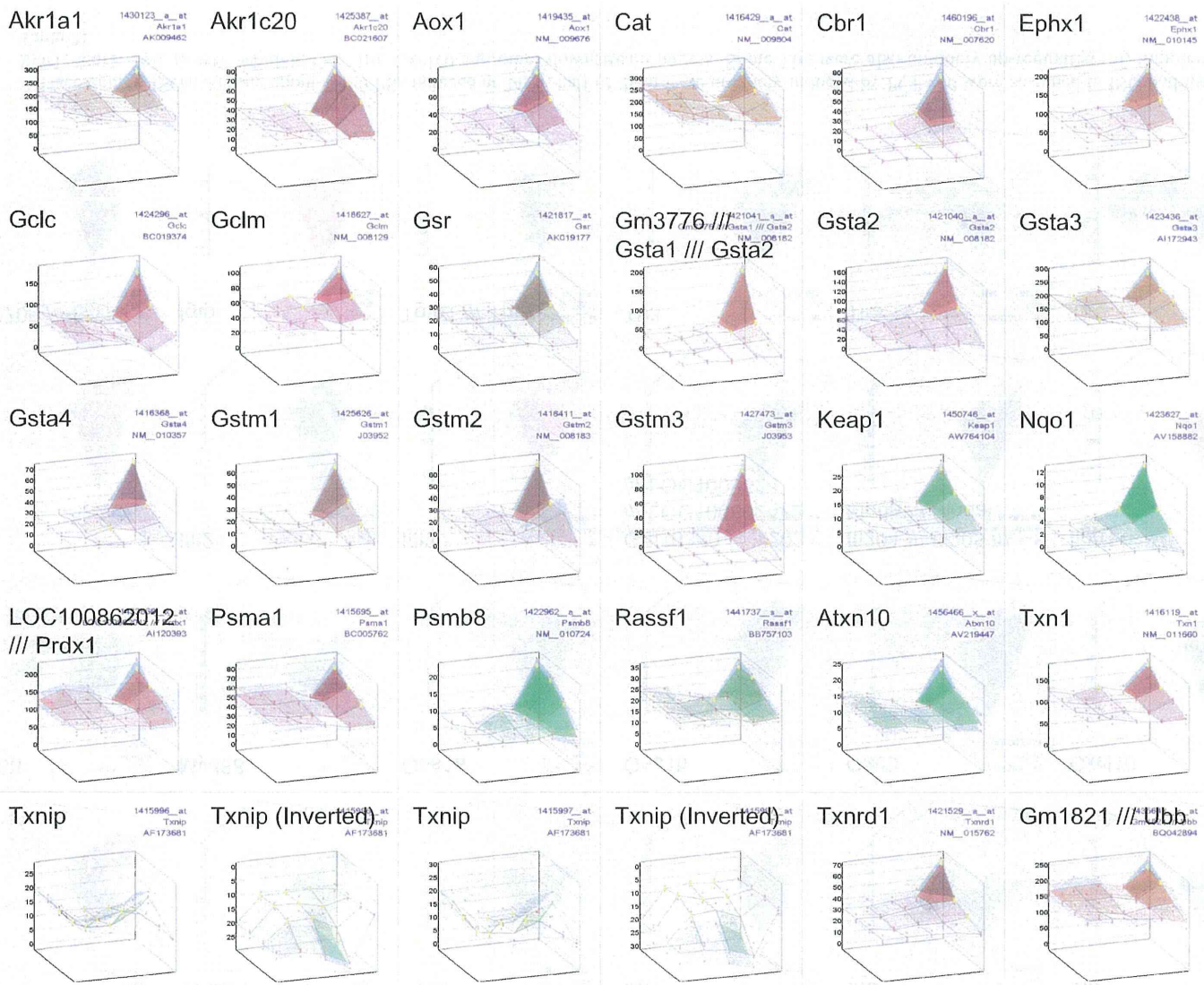

Fig. 5. Surface data of Nrf2-mediated oxidative stress response genes: Among about 1,200 PSs induced at 24 hr, another half of them were Nrf2-mediated oxidative stress response genes commonly induced by PCP and other 10 or so chemicals (cf. Supplementary Table 2). Nrf2 itself did not alter but Keap1 was clearly induced.

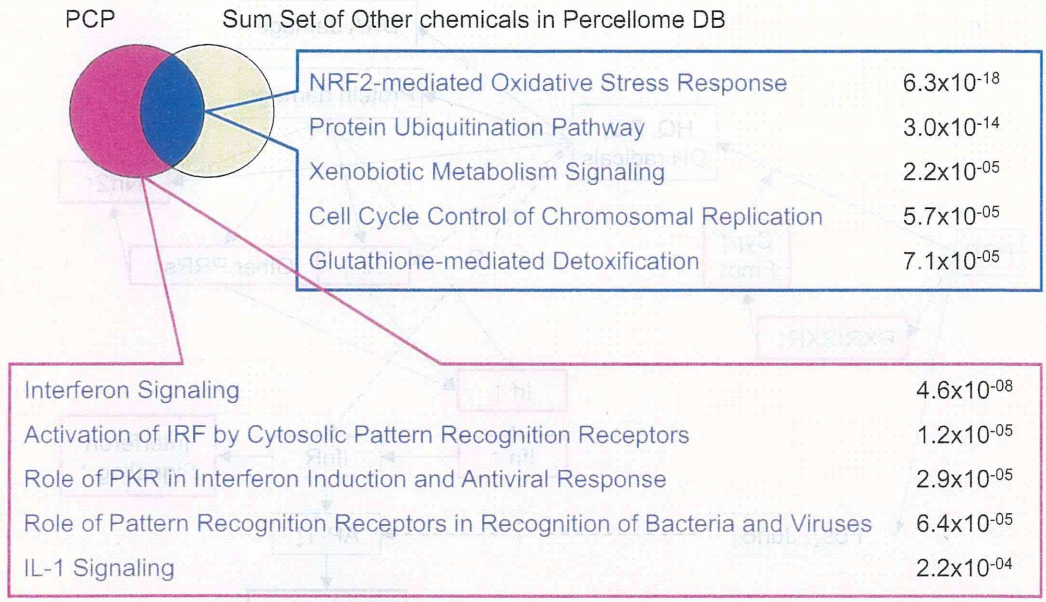

Fig. 6. Venn diagram of the PSs of PCP and sum set of other chemicals in Percellome Database. The PS list unique to PCP was assigned to Interferon signaling and related networks. The PSs induced by PCP and were shared by other chemicals in Percellome database were enriched in Nrf2-mediated oxidative stress response and Protein ubiquitination pathways. The names of the responses and their probability scores are generated by the Ingenuity Pathway analysis.

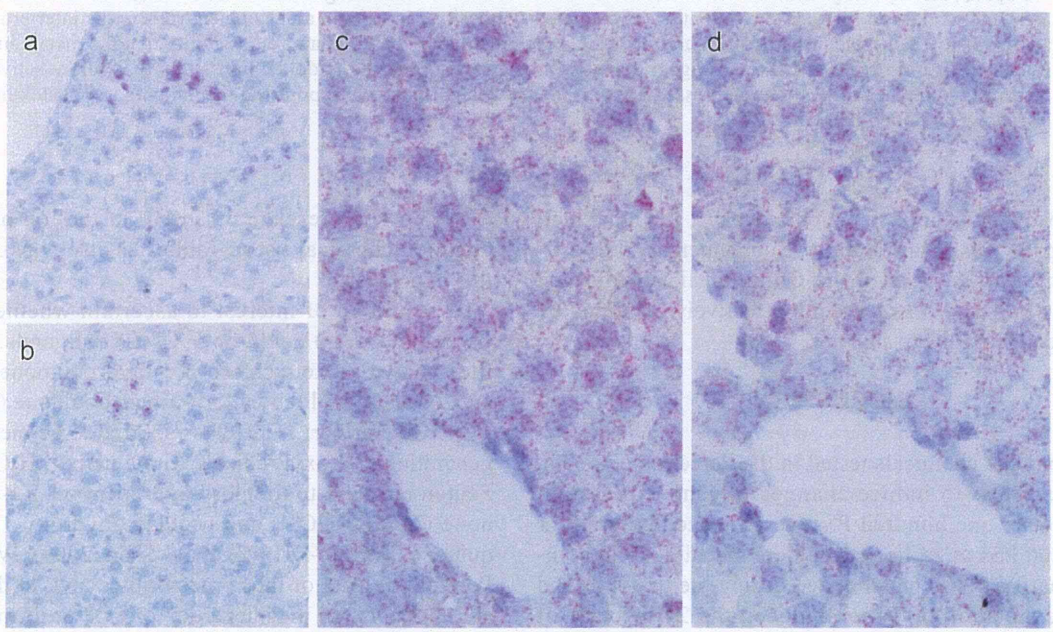

Fig. 7. *In situ* hybridization of Irf7 and Stat1. a) Vehicle control liver stained for Irf7. In a very low back ground, a small nest of hepatocytes was positively stained for Irf7. b) Vehicle control liver stained for Stat1. In a very low back ground, a small nest of hepatocytes was positively stained for Irf7. It is likely that the same hepatocyte is producing both mRNAs. c, d) High dose group stained for Irf7 and Stat1. Hepatocytes were shown to produce both mRNAs in a ubiquitous manner.

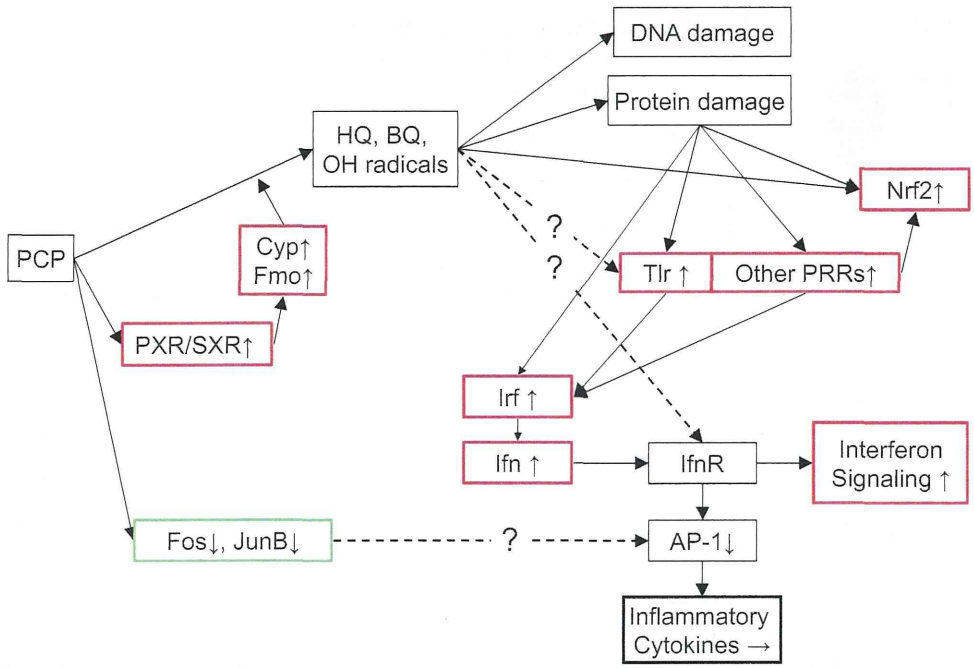

Fig. 8. Tentative summary scheme of the PCP induced networks in mouse liver. PCP or its metabolites may stimulate PXR/SXR or CAR, thereby inducing Cyp2, 4, 7, Fmo2, 5 within 8 hr to facilitate PCP metabolism, generating HQ (TCoHQ,TCpHQ), BQ (TCpBQ) and hydroxyl radical. The metabolites/radicals induce DNA damage and Protein damage. These reaction triggers Nrf2 networks and PRR system, initiating Irf mediated synthesis of Interferon alpha, which triggers the interferon signaling networks by autocrine or paracrine mechanisms. On the other hand, there remains a possibility that the metabolites may act as direct ligands to Tlr or IfnR and trigger downstream events as indicated in dotted lines with "?". Before activating interferon signaling networks, PCP suppressed Fos and JunB, which might have suppressed the inflammatory cytokine induction as shown in dotted line with "?".

accompanying distinct induction of Keap1, and other metabolic pathways (Figs. 5 and 6, Supplementary Table 1). Those networks were in the Common list mentioned above. Other networks were not effectively identified by the Ingenuity pathway analysis.

DISCUSSION

Among the chemicals tested in the Percellome project, PCP was slow to induce changes in gene expression; only around one hundred PSs were induced before 8 hr and 1,200 PSs at 24 hr. It would be plausible to hypothesize that PCP was metabolized during the first 8 hr and that the metabolite(s) then induced the 24 hr burst of ISGs and Nrf2-mediated genes. The time course of PCP action is in accord with the reported biological half-life of PCP; 6 to 27 hr in rodents (Larsen *et al.*, 1972; Braun *et al.*, 1977). A few metabolizing enzymes located downstream of PXR/SXR were induced during the first 8 hr (Fig. 3). The presence of DEHP in the top part of the common chemical list in Table 1 is also consistent with this hypothesis.

It would be of interest to ascertain whether PCP or its metabolite(s) could be PXR/SXR ligands. Metabolites known are tetrachloro-p(o)-hydroquinone (TCpHQ and TCoHQ) and tetrachloro-p-benzoquinone (chloranil, TCpBQ). Further, TCpHQ is reported to be metabolized, generating hydroxyl radicals with a help of H_2O_2 without Fenton reaction, to trichloro-hydroperoxyl-1,4-benzoquinone (TrCBQ-OOH) and trichloro-hydroxy-1,4-benzoquinone (TrCBQ-OH) (Zhu and Shan, 2009). We have no Percellome data of those metabolites and, to date, there are no reports on the interaction of PCP or its metabolites with the PXR/SXR. There are reports that PCP affects the function of estrogen receptor (Jung *et al.*, 2004) and thyroid hormone receptor (Kawaguchi *et al.*, 2008). Further study will be needed to identify the triggering event for the earliest responses to PCP.

Hepatocarcinogenic activity of PCP has been shown by rodent studies (NTP, 1999). The metabolites of PCP mentioned above were considered as the cause of oxidative stress or the hydroxyl radical insults against the liver (Zhu and Shan, 2009; Tasaki *et al.*, 2012).

It was reported that Tlr4-mediated, lipopolysaccharide-induced activation of the Ifn-β promoter was inhibited by PCP in a Myd88-independent way (Ohnishi *et al.*, 2008). On the other hand, PCP was considered to trigger Tlr4 via the induction of hydroxyl radicals (Lucas and Maes, 2013). In our experiment, PCP had significantly up-regulated Myd88, Irak1, Traf6, Tlr2, Tlr3, Tlr5, Tlr9 at 24 hr. Although the induction did not reach statistical significance, Tlr4 expression was also elevated. In addition, Irf 3, Irf7 and Irf9 were also induced. These findings might indicate that the TLR system was triggered by PCP itself, its metabolites or hydroxyl radicals via modifying the cytoplasmic proteins; abnormal proteins might be sensed by the TLRs or the pattern recognition receptors (PRR) system. Since Irf3, 7, 9 and Ifn-α1 expression are also increased, it could be possible that Irf mediated autocrine or paracrine of the Ifn-α is triggered, resulting in a burst of ISGs, as postulated by Sato *et al.* (Sato *et al.*, 2000).

Although Myd88 is mobilized, NF-κB, TNF, IL12 and CD40 were not induced, indicating that there may be a switch towards inflammatory cytokine production that was not directly induced by PCP. In relation to the switching mechanism, there is a report that isopropanol impaired AP-1 activation by removing Fos and JunB from the nuclear region of monocytes *in vitro* and suppressed Tlr4-mediated lipopolysaccharide stimulated Tnf-α production (Carignan *et al.*, 2011). In our data, Fos/JunB was down-regulated at earlier phase. As this change might correspond to AP-1 suppression (Gomard *et al.*, 2010), one possibility could be that PCP itself (as an alcohol/phenol) inhibited inflammatory cytokine production.

In contrast to the possible indirect mechanisms noted above, there are two examples that lead us to consider a possibility of direct activation of the ISGs. The first example is a low-molecular weight compound "imiquimod", a Tlr7 agonist, already on the market for treatment of skin viral infection (Hemmi *et al.*, 2002). Subcutaneous injection of imiquimod was reported to induce fever, sickness behavior and induction of ISG in rats (Damm *et al.*, 2012). The second example is a new polyfluoromethylated compound, 8-(1, 3,4-oxadiazol-2-yl)-2, 4-bis (trifluoromethyl) imidazo [1, 2-a] [1, 8] naphthyridine (RO4948191) which was reported to be an orally available low molecular weight interferon receptor agonist. RO4948191 was shown to induce a set of ISGs (Konishi *et al.*, 2012), such as Oas1, Adar, Bst1, Stat1, Ifit3, Usp18, Isg15, Herc6 and Cxcl10. These two examples of direct ligands to TLR and IFNR lead us to hypothesize that PCP and/or its metabolites may be able to directly activate these receptor systems (Fig. 8). Further investigation will be needed to clarify the molecular mechanism(s) through which PCP administration triggers the ISGs. It is tempting to speculate that this classic toxin, PCP, could be used as a new lead for orally applicable interferon-manipulating and/or cytokine switching drugs.

Hyperthermia or hyperpyrexia, profuse sweating, uncoordinated movement, muscle twitching, and coma are reported in humans and experimental animals as acute symptoms of PCP poisoning. These functional symptoms were reported to be caused by the mitochondrial uncoupling effect of PCP. Ucp2 and Ucp3 and some mitochondrial genes are induced in this study (Supplementary Table 2, Supplementary Fig 1). These genes are supportive for uncoupling effect. However, many of the Krebs cycle enzymes were not induced and those that were induced showed very small increases compared to the induction of ISGs. Some peroxidases were also mildly induced, but catalase was not induced by PCP. In the Percellome database, chemicals reported as uncouplers are aspirin, ethanol, sodium arsenite, and 2,4-dinitrophenol. Under the current computational condition, none of them was picked up as a chemical sharing PS list with PCP.

Taken together, our data may be interpreted to indicate that the functional symptoms represented by hyperthermia can be induced by PCP mainly through the activation of ISGs. This interpretation is backed up by the literature on "endogenous pyrogens" (Dinarello, 1999) and on imiquimod (Damm *et al.*, 2012).

Finally, although not yet perfected, the performance of the RSort and PE programs were demonstrated to be sufficient to sort out biologically meaningful changes for the comprehensive characterization of PCP. Manual searches employing different criteria added about 100 mildly changing PSs (data not shown), but the conclusions of our study were not affected. Nevertheless, further refinement for the better coverage is underway.

In conclusion, the RSort program-based comprehensive cross-reference of the Percellome database revealed that PCP was the only chemical among 111 orally administered chemicals that significantly induced the ISGs in hepatocytes. *In situ* hybridization confirmed that the parenchymal hepatocytes are responding to PCP. Two possible mechanisms were discussed; indirect mechanism via the PRR system, and direct stimulation of the Tlr(s) or IfnR(s). Further study is needed to clarify the possible molecular mechanisms.

ACKNOWLEDGMENTS

The author thanks all the member of the division of Cellular and Molecular Toxicology, NIHS for strong support of the project, and Dr. Bruce Blumberg for critical reading of the manuscript. The project has been supported by MHLW Health Sciences Research Grants H24-Kagaku-Shitei-006, H21-Kagaku-Ippan-001, H19-Toxico-001, H18-Kagaku-Ippan-001, H15-Kagaku-002, H14-Toxico-001, and H13-Seikatsu-012.

REFERENCES

Braun, W.H., Young, J.D., Blau, G.E. and Gehring, P.J. (1977): The pharmacokinetics and metabolism of pentachlorophenol in rats. Toxicol. Appl. Pharmacol., **41**, 395-406.

Carignan, D., Désy, O. and de Campos-Lima, P.O. (2011): The dysregulation of the monocyte/macrophage effector function induced by isopropanol is mediated by the defective activation of distinct members of the AP-1 family of transcription factors. Toxicol. Sci., **125**, 144-156.

Clayton, G.D. and Clayton, F.E. (1981): Toxicology. John Wiley Sons, New York.

Damm, J., Wiegand, F., Harden, L.M., Gerstberger, R., Rummel, C. and Roth, J. (2012): Fever, sickness behavior, and expression of inflammatory genes in the hypothalamus after systemic and localized subcutaneous stimulation of rats with the Toll-like receptor 7 agonist imiquimod. Neuroscience, **201**, 166-183.

Deichman, W., Machle, W., Kitzmiller, K.V. and Thomas, G. (1942): Acute and chronic effects of pentachlorophenol and sodium pentachlorophenate upon experimental animals. J. Pharmacol. Exp. Ther., **76**, 104-117.

Dinarello, C.A. (1999): Cytokines as endogenous pyrogens. J Infect Dis., **179 Suppl. 2**, S294-S304.

Finck, B.N., Gropler, M.C., Chen, Z., Leone, T.C., Croce, M.A., Harris, T.E., Lawrence, J.C.Jr. and Kelly, D.P. (2006): Lipin 1 is an inducible amplifier of the hepatic PGC-1alpha/PPARalpha regulatory pathway. Cell. Metab., **4**, 199-210.

Gomard, T., Michaud, H.A., Tempé, D., Thiolon, K., Pelegrin, M. and Piechaczyk, M. (2010): An NF-kappaB-dependent role for JunB in the induction of proinflammatory cytokines in LPS-activated bone marrow-derived dendritic cells. PLoS One, **5**, e9585.

Hemmi, H., Kaisho, T., Takeuchi, O., Sato, S., Sanjo, H., Hoshino, K., Horiuchi, T., Tomizawa, H., Takeda, K. and Akira, S. (2002): Small anti-viral compounds activate immune cells via the TLR7 MyD88-dependent signaling pathway. Nat. Immunol., **3**, 196-200.

Jung, J., Ishida, K. and Nishihara, T. (2004): Anti-estrogenic activity of fifty chemicals evaluated by in vitro assays. Life Sci., **74**, 3065-3074.

Kanno, J., Aisaki, K., Igarashi, K., Nakatsu, N., Ono, A., Kodama, Y. and Nagao, T. (2006): "Per cell" normalization method for mRNA measurement by quantitative PCR and microarrays. BMC Genomics, **7**. 64.

Kawaguchi, M., Morohoshi, K., Saita, E., Yanagisawa, R., Watanabe, G., Takano, H., Morita, M., Imai, H., Taya, K. and Himi, T. (2008): Developmental exposure to pentachlorophenol affects the expression of thyroid hormone receptor beta1 and synapsin I in brain, resulting in thyroid function vulnerability in rats. Endocrine, **33**, 277-284.

Konishi, H., Okamoto, K., Ohmori, Y., Yoshino, H., Ohmori, H., Ashihara, M., Hirata, Y., Ohta, A., Sakamoto, H., Hada, N., Katsume, A., Kohara, M., Morikawa, K., Tsukuda, T., Shimma, N., Foster, G.R., Alazawi, W., Aoki, Y., Arisawa, M. and Sudoh, M. (2012): An orally available, small-molecule interferon inhibits viral replication. Sci. Rep., **2**, 259.

Larsen, R.V., Kirsch, L.E., Shaw, S.M., Christian, J.E. and Born, G.S. (1972): Excretion and tissue distribution of uniformly labeled 14 C-pentachlorophenol in rats. J. Pharm. Sci., **61**, 2004-2006.

Lucas, K. and Maes, M. (2013): Role of the Toll Like Receptor (TLR) Radical Cycle in Chronic Inflammation: Possible Treatments Targeting the TLR4 Pathway. Mol. Neurobiol., (in press).

NTP (1999): NTP Toxicology and Carcinogenesis Studies of Pentachlorophenol (CAS NO. 87-86-5) in F344/N Rats (Feed Studies). In: Natl Toxicol Program Tech Rep Ser), pp.1-182.

Ohnishi, T., Yoshida, T., Igarashi, A., Muroi, M. and Tanamoto, K. (2008): Effects of possible endocrine disruptors on MyD88-independent TLR4 signaling. FEMS Immunol. Med. Microbiol., **52**, 293-295.

Puigserver, P., Rhee, J., Donovan, J., Walkey, C.J., Yoon, J.C., Oriente, F., Kitamura, Y., Altomonte, J., Dong, H., Accili, D. and Spiegelman, B.M. (2003): Insulin-regulated hepatic gluconeogenesis through FOXO1-PGC-1alpha interaction. Nature, **423**, 550-555.

Sato, M., Suemori, H., Hata, N., Asagiri, M., Ogasawara, K., Nakao, K., Nakaya, T., Katsuki, M., Noguchi, S., Tanaka, N. and Taniguchi, T. (2000): Distinct and essential roles of transcription factors IRF-3 and IRF-7 in response to viruses for IFN-alpha/beta gene induction. Immunity, **13**, 539-548.

Tasaki, M., Kuroiwa, Y., Inoue, T., Hibi, D., Matsushita, K., Ishii, Y., Maruyama, S., Nohmi, T., Nishikawa, A. and Umemura, T. (2012): Oxidative DNA damage and *in vivo* mutagenicity caused by reactive oxygen species generated in the livers of p53-proficient or -deficient gpt delta mice treated with non-genotoxic hepatocarcinogens. J. Appl. Toxicol. DOI: 10.1002/jat.2807.

Zhu, B.Z. and Shan, G.Q. (2009): Potential mechanism for pentachlorophenol-induced carcinogenicity: a novel mechanism for metal-independent production of hydroxyl radicals. Chem. Res. Toxicol., **22**, 969-977.

The web site for GeneChip data

The GeneChip data of PCP are accessible at http://www.nihs.go.jp/tox/TtgPublished.htm

Biochemical and Biophysical Research Communications 437 (2013) 579–584

Contents lists available at SciVerse ScienceDirect

Biochemical and Biophysical Research Communications

journal homepage: www.elsevier.com/locate/ybbrc

Autoimmune regulator, *Aire*, is a novel regulator of chondrocyte differentiation

Yuan Si [a], Kazuki Inoue [a,b,c], Katsuhide Igarashi [d], Jun Kanno [d], Yuuki Imai [a,c,*]

[a] Laboratory of Epigenetic Skeletal Diseases, Institute of Molecular and Cellular Biosciences, The University of Tokyo, Tokyo, Japan
[b] Department of Biological Resources, Integrated Center for Science, Ehime University, Ehime, Japan
[c] Division of Integrative Pathophysiology, Proteo-Science Center, Ehime University, Ehime, Japan
[d] Division of Cellular & Molecular Toxicology, Biological Safety Research Center, National Institute of Health Sciences, Tokyo, Japan

ARTICLE INFO

Article history:
Received 27 June 2013
Available online 11 July 2013

Keywords:
Chondrocyte differentiation
Aire
BMP2
Histone modification

ABSTRACT

Chondrocyte differentiation is controlled by various regulators, such as Sox9 and Runx2, but the process is complex. To further understand the precise underlying molecular mechanisms of chondrocyte differentiation, we aimed to identify a novel regulatory factor of chondrocyte differentiation using gene expression profiles of micromass-cultured chondrocytes at different differentiation stages. From the results of microarray analysis, the autoimmune regulator, Aire, was identified as a novel regulator. Aire stable knockdown cells, and primary cultured chondrocytes obtained from *Aire*$^{-/-}$ mice, showed reduced mRNA expression levels of chondrocyte-related genes. Over-expression of Aire induced the early stages of chondrocyte differentiation by facilitating expression of *Bmp2*. A ChIP assay revealed that Aire was recruited on an Airebinding site (T box) in the *Bmp2* promoter region in the early stages of chondrocyte differentiation and histone methylation was modified. These results suggest that Aire can facilitate early chondrocyte differentiation by expression of *Bmp2* through altering the histone modification status of the promoter region of *Bmp2*.

Taken together, Aire might play a role as an active regulator of chondrocyte differentiation, which leads to new insights into the regulatory mechanisms of chondrocyte differentiation.

1. Introduction

Chondrocyte differentiation is a process that establishes skeletal morphology during embryonic development as well as longitudinal growth after birth. Chondrocytes are differentiated from mesenchymal stem cells (MSCs), with subsequent differentiation into proliferative chondrocytes and then into hypertrophic chondrocyte [1,2]. This sequentialdifferentiation is regulated by various factors such as SRY-box containing gene 9 (Sox9), Indian hedgehog (Ihh), and parathyroid hormone-related protein (PTHrP) [1]. In early chondrocyte differentiation, Sox9, which is a crucial transcription factor mediated by Ihh/PTHrP and bone morphogenetic protein (BMP) signaling [3], regulates cartilage formation via upregulation of chondrocyte-specific genes such as *Col2a1* by cooperating with various proteins [4–6]. During the maturation stage, the expression of Sox9 can be down-regulated by RelA (a member of the NF-κB family). Subsequently, runt-related transcription factor 2 (Runx2) can induce differentiation into hypertrophic chondrocytes, which have high expression of *Col10a1* [7].

The mutation of the gene locus of these known factors can cause severe metaphyseal and/or epiphyseal dysplasias and chondrodysplasia [8–10]. However, the genes responsible for various osteochondrodysplasias and chondrocyte-related diseases remain elusive. It is necessary to understand the molecular mechanisms underlying chondrocyte differentiation for investigation into novel approaches to treat cartilage-related diseases. Consequently, identification of novel factors driving the process of chondrocyte differentiation, especially those related to epigenetic regulation, should be considered.

Epigenetic regulation is a mechanism that can control chromatin dynamics followed by transcriptional activation and repression [11]. Epigenetic regulations are mediated through reversible chemicalmodifications on DNA and histone proteins, and their recognition by various enzymes and nuclear proteins [12]. It has been reported that these epigenetic regulators play a significant role *in vivo* as well as *in vitro* [13–15]. However, epigenetic regulations in chondrocyte differentiation are still largely unknown. Thus, the purpose of this study was to identify novel transcription and/or epigenetic factors in chondrocyte differentiation in order to investigate the underlying molecular

* Corresponding author. Address: Division of Integrative Pathophysiology, Proteo-Science Center, Ehime University, Shitsugawa, Toon, Ehime 791-0295 Japan. Tel.: +81 89 960 5925; fax: +81 89 960 5953.
E-mail address: y-imai@m.ehime-u.ac.jp (Y. Imai).

0006-291X/$ - see front matter © 2013 Elsevier Inc. All rights reserved.
http://dx.doi.org/10.1016/j.bbrc.2013.07.001

mechanisms using an *in vitro* micromass culture system and gene expression microarrays.

2. Materials and methods

2.1. Animals

C57BL/6J mice were purchased from CLEA Japan (Tokyo, Japan) and *Aire*$^{-/-}$ mice were kindly provided from Dr. Mitsuru Matsumoto at Tokushima University, Japan [16]. All animals were maintained according to a protocol approved by the Animal Care and Use Committee of the University of Tokyo.

2.2. Chondrocytogenic cell culture

C3H10T1/2 cells were maintained in Dulbecco's Modified Eagle Medium (DMEM, Wako, Osaka, Japan) containing 10% fetal bovine serum (FBS, Nichirei Biosciences, Tokyo, Japan) and antibiotic–antimycotic (Gibco, USA) at 37 °C in an atmosphere of 5% CO_2. To induce chondrocyte differentiation, micromass-culturedC3H10T1/2 cells were treated with 100 ng/ml of recombinant human BMP2 (Osteopharma, Osaka, Japan) as previously reported [17]. Medium was changed every 2 days.

The early stage chondrogenic cell line, ATDC5, was maintained in DMEM/F12 (Gibco) with 5% FBS and antibiotic–antimycotic.

Primary chondrocytes were isolated from articular cartilage of postpartum mice at day 6 as previously reported [18]. The isolated chondrocytes were cultured at a density of 10^4 cells/well in a 24-well plate with 1.5 ml/well of DMEM (high glucose) with antibiotic–antimycotic and 10% FBS under sterile conditions in an atmosphere of 5% CO_2 at 37 °C. The culture medium was changed every 2 days. Cells were harvested at day 7 for RT-PCR.

2.3. Gene expression microarray analysis

Micromass-cultured cells were harvested at days 0, 5, 9 and 15, and gene expression microarrays were performed as described previously [19,20]. A heat map was generated with Multi Experiment Viewer software. Data were clustered and analyzed with DAVID bioinformatics database (http://david.abcc.ncifcrf.gov/) [21].

2.4. Real-time RT-PCR

Total RNA was extracted with Trizol (Invitrogen, USA) and was subsequently treated with DNase I (Takara BioInc., Otsu, Japan). First-strand cDNA was synthesized from total RNA using PrimeScript RT Master Mix (Takara Bio Inc.) and subjected to real-time RT-PCR using SYBR Premix Ex Tag II (Takara Bio Inc.) with Thermal Cycler Dice (Takara Bio Inc.) according to the manufacturer's instructions. Primers were purchased from Operon Biotechnologies (Tokyo, Japan) and the sequences of the primer sets are shown in Supplementary Table 1.

2.5. Immunohistochemistry (IHC)

Immunohistochemistry was performed as previously described [19]. Briefly, paraffin sections of decalcified tibiae of 9-week-old C57BL/6 mice were incubated overnight with primary antibodies (anti-Aire, LS-C29969, Lifespan, 1:1000 diluted by 2% goat serum in PBST) and then treated with a biotinylated secondary antibody (Vector Laboratories) and an avidin–biotin peroxidase complex (ABC Vectastain Kit, Vector). Diaminobenzidine tetrahydrochloride (Sigma) was the chromogen. Negative controls were prepared by omitting the primary antibody and replacing it with non-immune serum at the same dilution.

2.6. Establishment of Aire stable knockdown cell line

Knockdown experiments were performed as previously described [13]. Briefly, oligonucleotide sequences for short hairpin RNA (shRNA) targeting *Aire*, *Sox9* and *LacZ* were designed via BLOCK-iT™ RNAi designer (Invitrogen) and cloned into the pSUPER.reto.puro vector. Each vector was transfected into the Platinum-E cell line with lipofectamine2000 (Invitrogen). After 2 days,retrovirus was produced and infected into C3H10T1/2 cells with 10 μg/ml polybrene. 24 h later, cells were passaged and treated with puromycin (5 μg/ml) to select the infected cells. Culture medium was changed every 2 days. After 7 days, the stable knockdown cells were produced and the efficiency of knockdown was determined by real-time RT-PCR.

2.7. Luciferase reporter assay

A reporter plasmid was constructed using pGL3 (Promega) and 2 kb upstream from the transcriptional start site of the *Bmp2* gene. A reporter assay for the detection of transcriptional activity was performed with the Dual-Luciferase Reporter assay system (Promega). Approximately 80% confluent ATDC5 cells were transfected with *Bmp2* promoter–luciferase reporter plasmids with expression vectors of Aire. For evaluating transfection efficiency, the renilla-luciferase gene derived from the CMV promoter was used. Transfection was performed with Superfect transfection reagent (QIAGEN) according to the manufacturer's instructions. A dual luciferase assay was performed according to the manufacturer's instructions. In each experiment, firefly luciferase activity was normalized to renilla luciferase activity.

2.8. Chromatin immunoprecipitation (ChIP) assay

A ChIP assay was performed as described [13,22] with anti-Aire (ab13573, Abcam), anti-H3K4me2 (ab7766, Abcam) and normal goat or rabbit IgG as a control. Primer sets used for PCR were as follows: Aire binding T box site forward primer; 5′-CAAAACAGAAGC GTTTGCTCAC-3′, reverse primer;5′-TGGCCTCTGAGTTCCCTCATT-3′ and negative control site (about -5000 bp) forward primer; 5′-TCACTGGTACTTATGGCTGTGATG-3′, reverse primer; 5′-TCTGTGTT CCCTGCTCTGCT-3′.

2.9. Statistical analysis

We used one-way analysis of variance (ANOVA) to initially determine whether an overall statistically significant change existed before using Tukey's *post hoc* test and a two-tailed Student's *t* test to analyze the differences between two groups. For all graphs, data are represented as the mean ± S.D. Statistical significance was accepted at $p < 0.05$.

3. Results

3.1. Identification of the novel transcriptional factor, Aire, in chondrocyte differentiation

To identify novel transcriptional and/or epigenetic regulators in chondrocyte differentiation, micromass-cultured C3H10T1/2 cells were analyzed to establish chondrocyte differentiation *in vitro*. RT-PCR showed that *Col2a1* was highly expressed at day 5 and subsequently decreased, whereas the expression peak of *Col10a1* was detected at day 9 compared with other time points (Fig. 1A). This suggested that the micromass-cultured cells at days 0, 5 and 9 could be considered as MSCs, proliferative chondrocytes and hypertrophic chondrocytes, respectively.

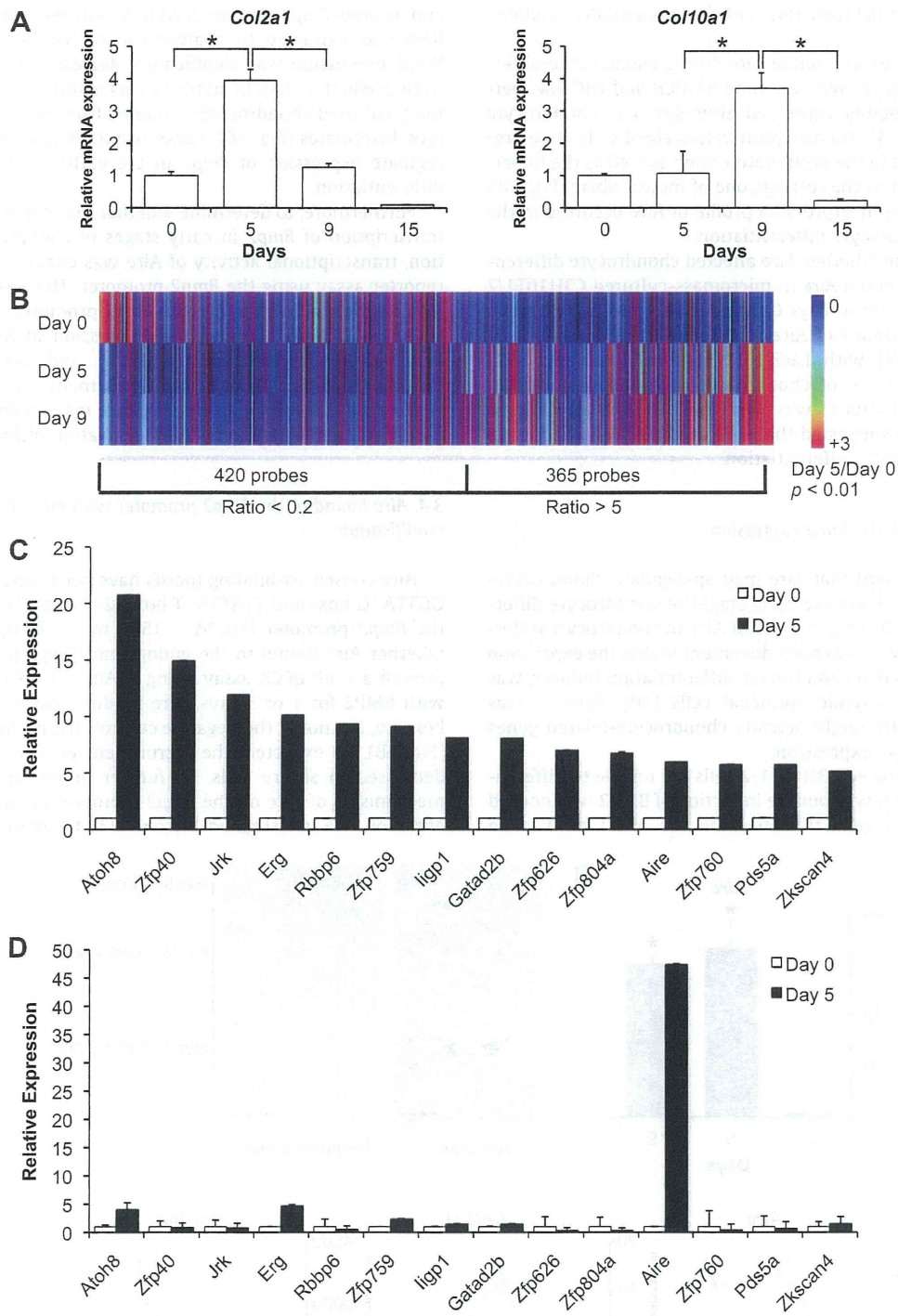

Fig. 1. Aire was identified as a novel transcriptional factor in chondrocyte differentiation. (A) Expression levels of *Col2a1* and *Col10a1* of micromass-cultured C3H10T1/2 cells treated with BMP2 for 0, 5, 9 and 15 days as determined by real-time RT-PCR and normalized to *Gapdh*. (B) A heat map of differentially expressed genes comparing day 0 and day 5. Genes with more than a 5-fold increase or 0.2-fold decrease as generated via Multi Experiment viewer software. (C) Expression levels of the genes categorized as "transcription" in the microarray. (D) Validation of microarray data by real-time RT-PCR and normalized to *Gapdh*. Data are presented as mean ± S.D. * indicates $p < 0.05$.

Based on the established pattern of chondrocyte differentiation, data from gene expression microarray showed a 5-fold significant difference of 785 genes (up-regulated: 365, down-regulated: 420) that were differentially expressed between day 0 and day 5 (Fig. 1B). All of them were clustered and analyzed based on the keyword "transcriptional factors" via the DAVID bioinformatics database and 14 factors were identified as possible candidates (Fig. 1C). After validation using real-time RT-PCR, the expression levels of *Aire* at day 5 were confirmed as the most significant increase compared to that at day 0 (Fig. 1D). Thus, Aire was suggested to be a novel transcription regulatory factor in chondrocyte differentiation.

3.2. Aire may activate the early stages of chondrocytedifferentiation

To determine the expression of Aire during chondrocyte differentiation *in vitro* and *in vivo*, real-time RT-PCR and IHC was performed. *Aire* was notably expressed after day 5 of chondrocyte differentiation (Fig. 2A) and Aire positively-stained cells were predominantly localized in the proliferative zone as well as the hypertrophic zone, but not in the resting zone of mouse tibiae (Fig. 2B). Therefore, the change in expression profile of Aire occurred in the early stages of chondrocyte differentiation.

Next, to determine whether Aire affected chondrocyte differentiation, we knocked down *Aire* in micromass-cultured C3H10T1/2 cells and harvested cells at days 0, 5 and 9 after BMP2 treatment. The knockdown efficiency of Aire-shRNA (sh*Aire*) was confirmed by RT-PCR compared with LacZ-shRNA (sh*LacZ*)-infected cells (Fig. 2C). The expression of chondrocyte differentiation marker genes (*Col2a1* and *Col10a1*) was decreased by *Aire* knockdown (Fig. 2C). These data suggested that Aire might be regarded as an activator of chondrocyte differentiation.

3.3. Aire may up-regulate Bmp2 expression

Our results suggested that Aire may up-regulate chondrocyte-related genes and promote the early stages of chondrocyte differentiation. However, the target genes of Aire in chondrocyte differentiation are unknown. Ithas been documented that the expression of *Bmp2*, the well-known chondrocyte differentiation inducer, was repressed in *Aire*$^{-/-}$ thymic epithelial cells [10]. Thus, it was hypothesized that Aire might activate chondrocyte-related genes via regulation of *Bmp2* expression.

As micromass-cultured C3H10T1/2 cells are unable to differentiate into chondrocytes without the induction of BMP2 we knocked down *Aire* in ATDC5 cells to determine the effect of Aire on endogenous *Bmp2*. At day 2, ATDC5 cells were harvested and the RNA was extracted to analyze the mRNA expression of *Bmp2*. *Bmp2* expression was significantly decreased in *Aire* knockdown ATDC5cells (Fig. 3A). In addition, this result was confirmed in primary cultured chondrocytes obtained from *Aire*$^{-/-}$ mice and wild-type littermates (Fig. 3B). These results indicated that Aire might regulate expression of *Bmp2* in the early stages of chondrocyte differentiation.

Furthermore, to determine whether Aire could directly regulate transcription of *Bmp2* in early stages of chondrocyte differentiation, transcriptional activity of Aire was examined by a luciferase reporter assay using the *Bmp2* promoter. The results showed that Aire could significantly increase *Bmp2* promoter activity in ATDC5 cells (Fig. 3C). In addition, overexpression of Aire could induce *Bmp2* expression as well as *Col2a1* and *Sox9* expression in C3H10T1/2 cells without BMP2 treatment (Fig. 3D). Taken together, these results indicate that Aire may facilitate chondrocyte differentiation via transcriptional activation of *Bmp2* expression.

3.4. Aire bound to the Bmp2 promoter with alteration of H3K4me2 modification

Aire consensus-binding motifs have been identified as the ATTGGTTA (G box) and TTATTA (T box) [23]. The T box motif exists in the *Bmp2* promoter (Fig.4A: −1503 to −1497 bp). To determine whether Aire bound to the endogenous *Bmp2* promoter, we performed a ChIP-qPCR assay using shAire C3H10T1/2 cells treated with BMP2 for 1 or 3 days. Aire binding was confirmed at the T box site, but not at the negative control site, in the *Bmp2* promoter (Fig. 4B). As expected, the recruitment of Aire was significantly decreased in shAire cells. To further understand the molecular mechanisms of Aire on the *Bmp2* promoter in chondrocyte differentiation, we investigated histone H3K4 modification, especially

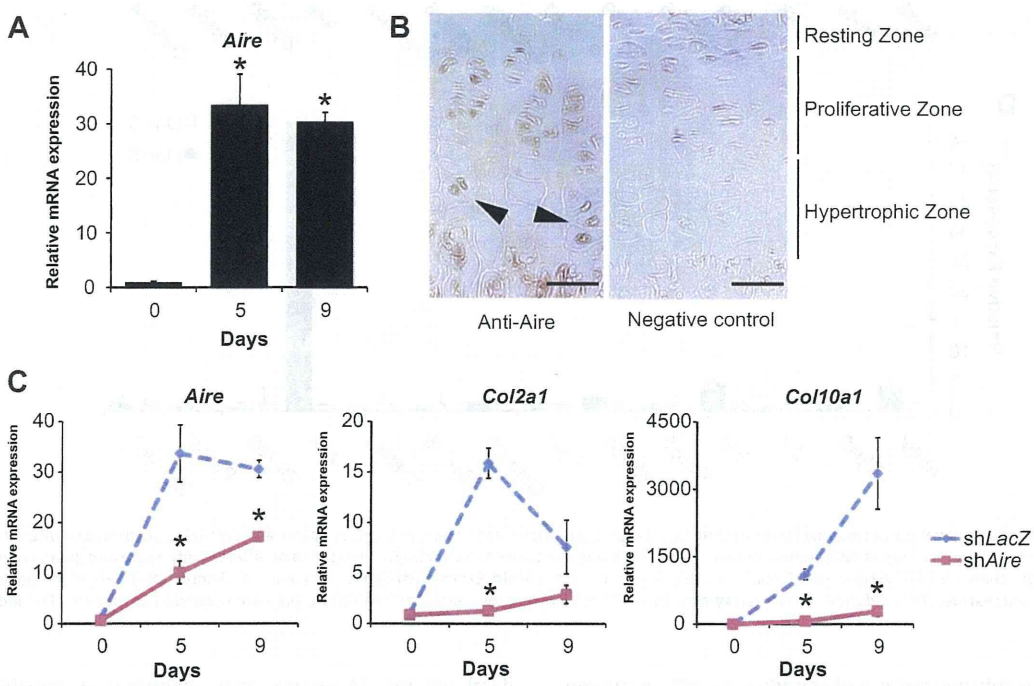

Fig. 2. Knockdown of *Aire* decreased the expression of chondrocyte-related genes. (A) Expression levels of *Aire* of micromass-cultured C3H10T1/2 cells treated with BMP2 for 0, 5 and 9 days as determined by real-time RT-PCR and normalized to *Gapdh*. (B) Immunohistochemistry of Aire in the proximal tibial growth plate. Immuno-positive cells stained in brown were localized in the proliferating zone and the hypertrophic zone (Arrow heads). The scale bar indicates 50 μm. (C) Expression levels of *Aire*, *Col2a1 and Col10a1* of micromass-cultured C3H10T1/2 cells treated with shAire or sh*LacZ* (negative control) and treated with BMP2 for 0, 5 and 9 days, as determined by real-time RT-PCR and normalized to *Gapdh*. Data are presented as mean ± S.D. * indicates $p < 0.05$. (For interpretation of the references to colour in this figure legend, the reader is referred to the web version of this article.)

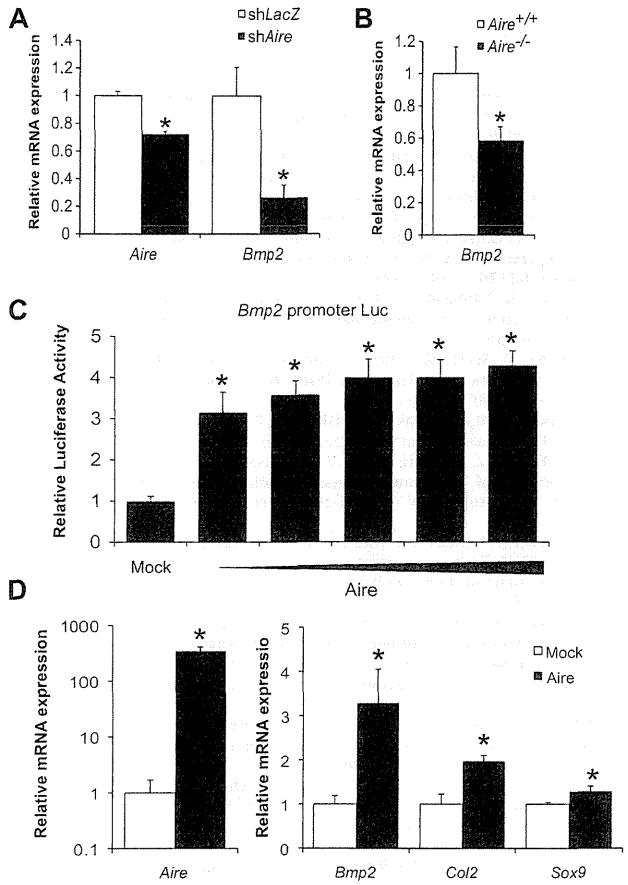

Fig. 3. Aire can facilitate chondrocyte differentiation by up-regulating *Bmp2* expression. (A) The expression of *Bmp2* was down-regulated by sh*Aire* in ATDC5 cells, as determined by real-time RT-PCR. (B) The expression levels of *Bmp2* in primary cultured chondrocytes obtained from *Aire*$^{-/-}$ mice was decreased compared to that of *Aire*$^{+/+}$ littermates, as determined by real-time RT-PCR. Data are presented as mean ± S.D. * indicates $p < 0.05$. (C) A luciferase assay was performed in ATDC5 cells transfected with the luciferase reporter vector (pGL3) including 2 kb of the *Bmp2* promoter and Aire expression vector (pcDNA3.1-Flag-Aire vector). Data are presented as mean ± S.D. * indicates $p < 0.05$ when compared to a mock transfection. (D) Expression levels of *Aire*, *Col2a1* and *Sox9* in micromass-cultured C3H10T1/2 cells without BMP2 treatment, as determined by real-time RT-PCR and normalized to *Gapdh*. Data are presented as mean ± S.D. * indicates $p < 0.05$.

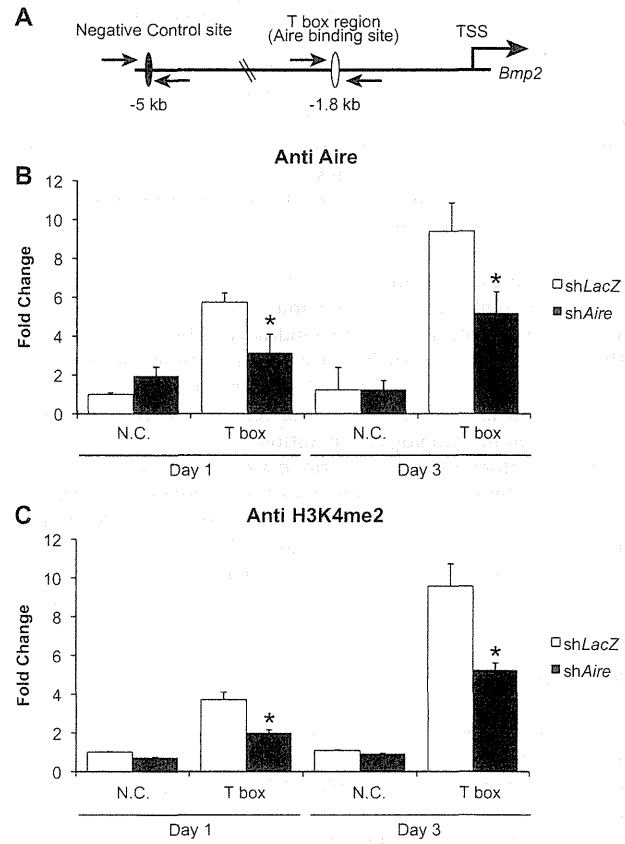

Fig. 4. Aire bound to the *Bmp2* promoter regulates *Bmp2* expression through histone H3K4 modification. (A) Schematic models of a ChIP assay for the T box and negative control sites (N.C.) in the *Bmp2* promoter region. A ChIP assay was performed using anti-Aire antibody (B) and anti-H3K4me2 antibody (C) for DNA extracted from micromass-cultured C3H10T1/2 cells treated with sh*Aire* or sh*LacZ* (negative control) and BMP2 for 1 and 3 days. Data were normalized by % input and are represented as mean ± S.D. * indicates $p < 0.05$.

the di-methylation of H3K4 since Aire contains a PHD zinc finger, which can recognize hypomethylated H3K4 [24]. As a result of a ChIP-qPCR assay, H3K4me2 was detected in the T box in the*Bmp2* promoter, and the modification levels were increased during chondrocyte differentiation. When Aire expression was knocked down, H3K4me2 levels at the T box site were decreased (Fig. 4C). Taken together, Aire may directly bind to the consensus Aire binding motif in the *Bmp2* promoter to regulate its expression through alteration of histone H3K4 methylation.

4. Discussion

In this study, we used gene expression microarrays to identify novel transcriptional and/or epigenetic factors in chondrocyte differentiation, which may give insight into the mechanism of chondrocyte differentiation. The microarray data showed that several differentially expressed genes exist during chondrocyte differentiation. In proliferative chondrocyte differentiation, the expression of Aire was significantly up-regulated. Analyses of *Aire* stable knockdown cells and *Aire*$^{-/-}$ primary cultured cells revealed that Aire may facilitate early stages of chondrocyte differentiation.

BMP2 a member of the transforming growth factor-βsuperfamily, plays a key role in inducing differentiation of MSCs into chondrocytes to form cartilage tissue via the BMP/Smad signaling pathway [25,26]. BMP2 is regulated by Gli2 in the sonic hedgehog signaling pathway. In this pathway, PI3-kinase/insulin-like growth factor can induce the expression of Gli2 [27]. Moreover, it has been documented that Aire is an active insulin regulator in thymus cells and *Bmp2* was repressed in *Aire*$^{-/-}$ thymic epithelial cells [28]. Based on this knowledge, we characterized the function of Aire on *Bmp2* expression in chondrocytes and found that Aire may play a role in the regulation of *Bmp2* expression through histone modification. These results were supported by previous reports, which suggested that the PHD1 domain of Aire can bind to hypomethylated H3K4 to concentrate Aire in binding regions and then activate the expression of target genes in mammary epithelial cells (MECs) [29].

Aire consists of a PHD zinc finger, but no significant domains harboring methyltransferase activities. However, a ChIP assay revealed that knockdown of Aire could decrease H3K4me2 levels at the Tbox site in the *Bmp2* promoter region. This alteration can be caused by histone modifiers, which interact with Aire on chromatin. It has been demonstrated that the PHD zinc finger of Aire can recognize hypomethylated histone H3 N-terminal tails to recruit transcriptional co-regulators including histone modifiers [24]. Identification of components of the Aire complex by biochemical purification may lead to comprehension of the precise molecular

mechanisms in the regulation of *Bmp2* expression by Aire during early chondrocyte differentiation.

Aire$^{-/-}$ mice did not exhibit significant abnormal phenotypes in skeletal morphology [28]. However, patients with mutations at the*AIRE* gene locus suffer from autoimmune polyendocrinopathy candidiasis ectodermal dystrophy (APECED) and some of them show reversible metaphyseal dysplasia (RMD) with notable progressive growth and abnormal endochondral ossification in adolescents [30]. *Cst10*$^{-/-}$ mice developed and grew normally but showed abnormal phenotypes in formation of osteoarthritic osteophytes, age-related ectopic ossification and healing of bone fractures [31]. Our current study and previous reports suggest that Aire might play an important role in chondrocyte differentiation during pathological conditions such as fracture healing or osteoarthritis development. Induction of skeletal diseases into *Aire*$^{-/-}$ mice will help to further understand the precise roles of Aire in chondrocyte differentiation in pathological conditions.

Taken together, we have identified a novel regulatory factor in chondrocyte differentiation, Aire, which can modify *Bmp2* expression though alteration of the epigenetic status of the *Bmp2* promoter region. This investigation may open the window for the development of therapeutic strategies against diseases related to chondrocyte differentiation, such as osteoarthritis or fracture healing.

Acknowledgments

We would like to thank Prof. Mitsuru Matsumoto at Tokushima University, Japan for providing us the *Aire* knockout mice andOsteopharma for providing us rhBMP2 We also thank Ms. Noriko Moriyama at National Institute of Health Sciences, Tokyo, Japan, for her technical support (microarray). This work was supported by JSPS KAKENHI Grant Number 23689066 to Y.I.

Appendix A. Supplementary data

Supplementary data associated with this article can be found, in the online version, at http://dx.doi.org/10.1016/j.bbrc.2013.07.001.

References

[1] H.M. Kronenberg, Developmental regulation of the growth plate, Nature 423 (2003) 332–336.
[2] O. Nilsson, D. Chrysis, I. Pajulo, A. Boman, M. Holst, J. Rubinstein, E.M. Ritzen, L. Savendahl, Localization of estrogen receptors-alpha and -beta and androgen receptor in the human growth plate at different pubertalstages, J. Endocrinol. 177 (2003) 319–326.
[3] J. Kramer, C. Hegert, K. Guan, A.M. Wobus, P.K. Muller, J. Rohwedel, Embryonic stem cell-derived chondrogenic differentiation in vitro: activation by BMP-2 and BMP-4, Mech.Dev. 92 (2000) 193–205.
[4] K. Hata, R. Nishimura, S. Muramatsu, A. Matsuda, T. Matsubara, K. Amano, F. Ikeda, V.R. Harley, T. Yoneda, Paraspeckle protein p54nrb links Sox9-mediated transcription withRNA processing during chondrogenesis in mice, J. Clin. Invest. 118 (2008) 3098–3108.
[5] K. Amano, K. Hata, S. Muramatsu, M. Wakabayashi, Y. Takigawa, K. Ono, M. Nakanishi, R. Takashima, M. Kogo, A. Matsuda, R. Nishimura, T. Yoneda, Arid5acooperates with Sox9 to stimulate chondrocyte-specific transcription, Mol. Biol. Cell. 22 (2011) 1300–1311.
[6] Y. Takigawa, K. Hata, S. Muramatsu, K. Amano, K. Ono, M. Wakabayashi, A. Matsuda, K. Takada, R. Nishimura, T. Yoneda, The transcription factor Znf219 regulates chondrocytedifferentiation by assembling a transcription factory with Sox9, J. Cell Sci. 123 (2010) 3780–3788.
[7] M. Ushita, T. Saito, T. Ikeda, F. Yano, A. Higashikawa, N. Ogata, U. Chung, K. Nakamura, H. Kawaguchi, Transcriptional induction of SOX9 by NF-κB family member RelA inchondrogenic cells, Osteoarthritis Cartilage 17 (2009) 1065–1075.
[8] J. Spranger, A. Winterpacht, B. Zabel, The type II collagenopathies: a spectrum of chondrodysplasias, Eur. J. Pediatr. 153 (1994) 56–65.
[9] T. Wagner, J. Wirth, J. Meyer, B. Zabel, M. Held, J. Zimmer, J. Pasantes, F.D. Bricarelli, J. Keutel, E. Hustert, U. Wolf, N. Tommerup, W. Schempp, G. Scherer, Autosomal sex reversal and campomelic dysplasia are caused by mutations in and around the SRY-related gene SOX9, Cell 79 (1994) 1111–1120.
[10] J.W. Foster, M.A. Dominguez-Steglich, S. Guioli, C. Kwok, P.A. Weller, M. Stevanovic, J. Weissenbach, S. Mansour, I.D. Young, P.N. Goodfellow, et al., Campomelic dysplasia and autosomal sex reversal caused by mutations in an SRY-related gene, Nature 372 (1994) 525–530.
[11] M.G. Rosenfeld, V.V. Lunyak, C.K. Glass, Sensors and signals: a coactivator/corepressor/epigenetic code for integrating signal-dependent programs of transcriptional response, Genes Dev. 20 (2006) 1405–1428.
[12] R.K. Prinjha, J. Witherington, K. Lee, Place your BETs: the therapeutic potential of bromodomains, Trends Pharmacol. Sci. 33 (2012) 146–153.
[13] Y. Okuno, F. Ohtake, K. Igarashi, J. Kanno, T. Matsumoto, I. Takada, S. Kato, Y. Imai, Epigenetic regulation of adipogenesis by PHF2 histone demethylase, Diabetes 62 (2013) 1426–1434.
[14] Y. Okada, K. Yamagata, K. Hong, T. Wakayama, Y. Zhang, A role for the elongator complex in zygotic paternal genome demethylation, Nature 463 (2010) 554–558.
[15] Y. Okada, G. Scott, M.K. Ray, Y. Mishina, Y. Zhang, Histone demethylase JHDM2A is critical for Tnp1 and Prm1 transcription and spermatogenesis, Nature 450 (2007) 119–123.
[16] N. Kuroda, T. Mitani, N. Takeda, N. Ishimaru, R. Arakaki, Y. Hayashi, Y. Bando, K. Izumi, T. Takahashi, T. Nomura, S. Sakaguchi, T. Ueno, Y. Takahama, D. Uchida, S. Sun, F. Kajiura, Y. Mouri, H. Han, A. Matsushima, G. Yamada, M. Matsumoto, Development of autoimmunity against transcriptionally unrepressed target antigen in the thymus of Aire-deficient mice, J. Immunol. 174 (2005) 1862–1870.
[17] A.E. Denker, A.R. Haas, S.B. Nicoll, R.S. Tuan, Chondrogenic differentiation of murine C3H10T1/2 multipotential mesenchymal cells: i. stimulation by bone morphogenetic protein-2 in high-density micromass cultures, Differentiation 64 (1999) 67–76.
[18] M.C. Louie, H.Q. Yang, A.H. Ma, W. Xu, J.X. Zou, H.J. Kung, H.W. Chen, Androgen-induced recruitment of RNA polymerase II to a nuclear receptor-p160 coactivator complex, Proc. Natl. Acad. Sci.USA 100 (2003) 2226–2230.
[19] T. Nakamura, Y. Imai, T. Matsumoto, S. Sato, K. Takeuchi, K. Igarashi, Y. Harada, Y. Azuma, A. Krust, Y. Yamamoto, H. Nishina, S. Takeda, H. Takayanagi, D. Metzger, J. Kanno, K. Takaoka, T.J. Martin, P. Chambon, S. Kato, Estrogenprevents bone loss via estrogen receptor alpha and induction of Fas ligand in osteoclasts, Cell 130 (2007) 811–823.
[20] J. Kanno, K. Aisaki, K. Igarashi, N. Nakatsu, A. Ono, Y. Kodama, T. Nagao, "Per cell" normalization method for mRNA measurement by quantitative PCR and microarrays, BMCGenomics 7 (2006) 64.
[21] W. Huang da, B.T. Sherman, R.A. Lempicki, Systematic and integrative analysis of large gene lists using DAVID bioinformatics resources, Nat. Protoc. 4 (2009) 44–57.
[22] Q.G. Ruan, K. Tung, D. Eisenman, Y. Setiady, S. Eckenrode, B. Yi, S. Purohit, W.P. Zheng, Y. Zhang, L. Peltonen, J.X. She, The autoimmune regulator directly controls the expression of genes critical for thymic epithelial function, J. Immunol. 178 (2007) 7173–7180.
[23] P.G. Kumar, M. Laloraya, C.Y. Wang, Q.G. Ruan, A. Davoodi-Semiromi, K.J. Kao, J.X. She, The autoimmune regulator (AIRE) is a DNA-binding protein, J. Biol.Chem. 276 (2001) 41357–41364.
[24] T. Org, F. Chignola, C. Hetenyi, M. Gaetani, A. Rebane, I. Liiv, U. Maran, L. Mollica, M.J. Bottomley, G. Musco, P. Peterson, The autoimmune regulator PHD finger binds to non-methylated histone H3K4 to activate gene expression, EMBO Rep. 9 (2008) 370–376.
[25] D. Chen, M. Zhao, G.R. Mundy, Bone morphogenetic proteins, Growth Factors 22 (2004) 233–241.
[26] T. Sakou, T. Onishi, T. Yamamoto, T. Nagamine, T.K. Sampath, P. Ten Dijke, Localization of smads, the TGF-beta family intracellular signaling components during endochondral ossification, J. Bone Miner. Res. 14 (1999) 1145–1152.
[27] M. Zhao, M. Qiao, S.E. Harris, D. Chen, B.O. Oyajobi, G.R. Mundy, The zinc finger transcription factor Gli2 mediates bone morphogenetic protein 2 expression in osteoblasts in response to hedgehog signaling, Mol. Cell. Biol. 26 (2006) 6197–6208.
[28] A.S. Koh, A.J. Kuo, S.Y. Park, P. Cheung, J. Abramson, D. Bua, D. Carney, S.E. Shoelson, O. Gozani, R.E. Kingston, C. Benoist, D. Mathis, Aire employs a histone-binding module to mediate immunological tolerance, linking chromatin regulation with organ-specific autoimmunity, Proc. Natl. Acad. Sci. USA 105 (2008) 15878–15883.
[29] B. Shu, M. Zhang, R. Xie, M. Wang, H. Jin, W. Hou, D. Tang, S.E. Harris, Y. Mishina, R.J. O'Keefe, M.J. Hilton, Y. Wang, D. Chen, BMP2, but not BMP4, is crucial for chondrocyte proliferation and maturation during endochondral bone development, J. Cell Sci. 124 (2011) 3428–3440.
[30] M. Harris, O. Kecha, C. Deal, C.R. Howlett, D. Deiss, V. Tobias, J. Simoneau-Roy, J. Walker, Reversible metaphyseal dysplasia, a novel bone phenotype, in two unrelated children with autoimmunepolyendocrinopathy-candidiasis-ectodermal dystrophy: clinical and molecular studies, J. Clin. Endocrinol. Metab. 88 (2003) 4576–4585.
[31] T. Yamada, H. Kawano, Y. Koshizuka, T. Fukuda, K. Yoshimura, S. Kamekura, T. Saito, T. Ikeda, Y. Kawasaki, Y. Azuma, S. Ikegawa, K. Hoshi, U.I. Chung, K. Nakamura, S. Kato, H. Kawaguchi, Carminerin contributes to chondrocyte calcification during endochondral ossification, Nat. Med. 12 (2006) 665–670.

The Journal of Toxicological Sciences (J. Toxicol. Sci.)
Vol.38, No.2, 279-283, 2013

Letter

Neonatal exposure to 2,3,7,8-tetrachlorodibenze-p-dioxin increases the mRNA expression of prostatic proteins in C57BL mice

Nariaki Fujimoto[1], Atsuya Takagi[2] and Jun Kanno[2]

[1]Endocrine Research Group, Department of Disease Model, Research Institute for Radiation Biology and Medicine, Hiroshima University, 1-2-3 Kasumi, Minami-ku, Hiroshima 734-8553, Japan
[2]Division of Toxicology, National Institute of Health Sciences, Kamiyoga 1-18-1, Setagaya-ku, Tokyo 158-8501, Japan

(Received January 9, 2013; Accepted February 9, 2013)

ABSTRACT — The effects of neonatal exposure to low doses of 2,3,7,8-tetrachlorodibenzo-p-dioxin (TCDD) on prostatic secretory protein expression were investigated. Male C57BL mice were treated with TCDD at 10, 100, or 1,000 ng/kg body weight at postnatal day (PND) 6. At PND42, the ventral, dorsolateral, and anterior prostatic lobes were dissected and the mRNA expression of prostatic proteins including spermine-binding protein, serine protease inhibitor Kazal type 3, prostate secretory protein 94 (PSP94), immunoglobulin binding protein-like protein (IgGBPLP), experimental autoimmune prostatitis antigen proteins, and peroxiredoxin-6 (Prdx6) was measured by quantitative PCR. There was no significant difference in the weight of the prostatic lobes between the control and TCDD-treated groups. The expression of PSP94 and Prdx6 in the ventral prostate and IgGBPLP in the dorsolateral prostate at PND42 was significantly increased by neonatal TCDD treatment in a dose-dependent manner, while no changes were noted in other prostatic secretions. These data suggest that neonatal exposure to TCDD may have effects on the neonatal differentiation of the prostate and results in the hyper-expression of some prostatic proteins later in life.

Key words: 2,3,7,8-Tetrachlorodibenzo-p-dioxin (TCDD), Prostatic secretion, Mouse prostate, Neonatal effects

INTRODUCTION

The developing male reproductive system of laboratory rodents is highly sensitive to 2,3,7,8-tetrachlorodibenzo-p-dioxin (TCDD) (Mably *et al.*, 1992; Roman and Peterson, 1998; Theobald *et al.*, 2000). Its toxic effects include a decrease in the weight of the testis and accessory sex organs, degeneration of germ cells, and decreased spermatogenesis. The adverse effects of maternal exposure to TCDD on the development of the prostate gland have been studied extensively in rats and mice. In Holtzman rats, a single maternal dose of 64 ng/kg body weight (bw) of TCDD caused a significant decrease in ventral prostate (VP) weight (Mably *et al.*, 1992). More recently, it was reported that androgen receptor (AR) mRNA expression was reduced in the VP of Holtzman rats following maternal treatment with as low as 12.5 ng/kg bw TCDD (Ohsako *et al.*, 2001). In the mouse, the C57BL/6J strain appears to be sensitive to TCDD, in which the maternal administration of 5 μg/kg bw TCDD suppressed the development of the VP in the offspring, while the weight of the dorsolateral prostate (DLP) and anterior prostate (AP) decreased by approximately 50% (Lin *et al.*, 2002a). Exposure to TCDD during only the lactational period also resulted in offspring with lower prostate weights, but with less severe changes (Lin *et al.*, 2002b).

Although the previous studies have been clearly demonstrated that TCDD affect the development of the prostate morphologically, it is important to examine the effect on the prostatic function, production of prostatic proteins. We recently reported the identification of the major proteins secreted from the mouse prostate (Fujimoto *et al.*, 2006). The secreted proteins included spermine-binding protein (SBP), serine protease inhibitor Kazal type 3

Correspondence: Nariaki Fujimoto (E-mail: nfjm@hiroshima-u.ac.jp)

(SPI-KT3), prostate secretory protein 94 (PSP94), glucose-regulated protein, 78kDa (GRP78), peroxiredoxin-6 (Prdx6), probasin, experimental autoimmune prostatitis antigen protein (EAPA2), and immunoglobulin binding protein-like protein (IgGBPLP). The expression profile of these proteins would be useful for studying prostatic function and may also provide markers for evaluating the effects of environmental chemicals on the prostate. In the present study, we investigated the effects of neonatal exposure to low doses of TCDD on the mRNA expression of prostatic proteins as well as AR in the prostate.

MATERIALS AND METHODS

Animal experiments

The animal experiments were conducted under the approval of the Animal Experiment Committee of the National Institute of Health Sciences (NIHS). All experiments involving TCDD-treated animals were carried out following the rules for the use of TCDD set by NIHS. Five-day-old male C57BL mice were purchased from Charles River Japan Co. and maintained with free access to a basal diet and tap water. At postnatal day (PND) 6, the animals were divided into 4 groups (n = 6, each group): control and 3 TCDD-treated groups. TCDD (Cambridge Isotope Laboratories, Inc., Andover, MA, USA) in corn oil (50 μl) was injected intraperitoneally (ip) at doses of 0, 10, 100, or 1,000 ng/kg bw). At PND42, the animals were killed under ether anesthesia, since our previous study indicated that the mRNA expression of prostatic proteins is matured at PND42 (Fujimoto *et al.*, 2006). The prostatic lobes were dissected under a microscope, then immediately fixed in RNAlater Solution (Life technologies, Grand Island, NY, USA).

Quantification of mRNA by real-time RT-PCR

Total RNA was prepared from prostatic tissues using an RNA isolation kit (NucleoSpin RNA II; Machery-Nagel GmbH & Co. KG, Düren, Germany). An ABI Prism 7500 (Applied Biosystems/Life Technologies Co., Carlsbad, CA, USA) was employed for the RT-PCR based quantification of prostatic protein mRNAs as described previously (Fujimoto *et al.*, 2006). All mRNA levels were normalized with reference to β-actin mRNA.

Statistical analysis

Statistical comparisons were made by Dunnett's multiple comparison test.

RESULTS

Body and prostate lobe weights

There was no significant difference in body weight between the control and 3 TCDD-treated groups at PND42 (Table 1). There was no significant change in the weight of either the VP, DLP, or AP.

Expression of prostatic protein and AR mRNAs

SBP and SPI-KT3 were preferentially expressed in the VP, while probasin, EAPA2, and IgGBPLP expression was localized in the DLP and AP (Table 2). PSP94 was expressed in both the VP and DLP, while GRP78 and Prdx6 were expressed in all prostatic lobes. The effects of neonatal treatment of TCDD on mRNA expression were evident for PSP94, Prdx6, and IgGBPLP. The effects were lobe specific; that is, neonatal TCDD increased the expression of PSP94 and Prdx6 mRNA in the VP as well as IgGBPLP mRNA in the DLP in a dose-dependent manner. Neonatal TCDD exposure did not change the expression of AR mRNA in the VP or DLP, but decreased its expression in the AP.

DISCUSSION

Maternal exposure to TCDD reportedly causes irreversible changes to the reproductive systems of offspring, including reduced sperm count and reduced size of the reproductive organs. The development of the male reproductive organs in rodents, in particular the prostate gland, has been recognized as a sensitive target to

Table 1. Weight of body and prostatic lobes at PND42

Treatment	body weight (g)	VP (mg/g bw)	DLP (mg/g bw)	AP (mg/g bw)
control	16.8 ± 0.28	0.20 ± 0.03	0.21 ± 0.02	0.30 ± 0.02
TCDD 10	16.9 ± 0.37	0.19 ± 0.02	0.23 ± 0.01	0.22 ± 0.06
TCDD 100	17.7 ± 0.25	0.30 ± 0.08	0.20 ± 0.02	0.34 ± 0.03
TCDD 1000	18.9 ± 0.38	0.24 ± 0.08	0.24 ± 0.01	0.31 ± 0.03

Mean ± S.E.M. (n = 6). Male C57BL mice were treated with TCDD (10, 100, or 1,000 ng/kg bw) at postnatal day (PND) 6 and sacrificed at PND42.

Table 2. mRNA expression of prostatic proteins and AR in prostatic lobes

Treatment	SBP	SPI-KT3	PSP94	GRP78	Prdx6	Probasin	EAPA2	IgGBPLP	AR
VP									
control	315 ± 64.4	280 ± 85.7	12.4 ± 4.2	5.7 ± 0.36	1.5 ± 0.21				7.3 ± 1.24
TCDD 10	293 ± 131.2	495 ± 95.7	40.0 ± 11.9	7.6 ± 0.92	2.4 ± 0.38				8.6 ± 1.08
TCDD 100	322 ± 63.6	278 ± 44.1	65.7 ± 21.1*	8.3 ± 1.89	4.5 ± 0.79*				4.8 ± 0.27
TCDD 1000	450 ± 84.7	308 ± 46.5	110 ± 16.6**	7.1 ± 1.68	5.6 ± 1.0*				7.5 ± 0.71
DLP									
control			92.3 ± 20.2	11.2 ± 1.23	27.2 ± 4.7	7.8 ± 0.65	2.5 ± 0.44	0.80 ± 0.09	4.5 ± 0.96
TCDD 10			59.0 ± 24.3	9.5 ± 1.21	31.7 ± 1.93	9.1 ± 1.36	2.8 ± 0.44	2.2 ± 0.59	3.9 ± 0.45
TCDD 100			82.3 ± 20.7	8.9 ± 1.07	31.6 ± 3.02	8.5 ± 0.57	2.4 ± 0.29	2.7 ± 0.75*	3.5 ± 0.22
TCDD 1000			56.9 ± 15.9	7.3 ± 0.71	31.3 ± 2.46	7.9 ± 0.07	2.5 ± 0.28	3.3 ± 0.47*	3.2 ± 0.50
AP									
control				13.7 ± 3.23	38.1 ± 5.4	4.5 ± 0.66	3.4 ± 0.29	19.5 ± 1.95	3.6 ± 0.35
TCDD 10				18.0 ± 1.59	67.1 ± 4.1	5.8 ± 0.21	3.0 ± 0.33	27.8 ± 5.63	3.0 ± 0.31
TCDD 100				9.8 ± 0.91	40.9 ± 6.13	3.9 ± 0.52	3.0 ± 0.57	11.2 ± 1.90	1.9 ± 0.22
TCDD 1000				14.6 ± 1.90	73.6 ± 15.4	5.9 ± 0.75	3.3 ± 0.37	28.3 ± 6.19	2.1 ± 0.32

Mean ± S.E.M. (n = 5 or 6). Values are mRNA levels divided by beta actin mRNA levels (*$p < 0.05$ and **$p < 0.01$ vs. control).
Male C57BL mice were treated with TCDD (10, 100, or 1,000 ng/kg body weight) at postnatal day (PND) 6 and sacrificed at PND42.